ACS APPLIED MATERIALS & INTERFACES

Review

www.acsami.org

Visibly Transparent Heaters

Ritu Gupta,*[,†] K. D. M. Rao,[‡] S. Kiruthika,[§] and Giridhar U. Kulkarni*[,‡,⊥]

[†]Department of Chemistry, Indian Institute of Technology Jodhpur, Jodhpur 342011, Rajasthan, India

[‡]Centre for Nano and Soft Matter Sciences, Jalahalli, Bangalore 560013, India

[§]Chemistry & Physics of Materials Unit and Thematic Unit of Excellence in Nanochemistry, Jawaharlal Nehru Centre for Advanced Scientific Research, Jakkur P.O., Bangalore 560064, India

ABSTRACT: Heater plates or sheets that are visibly transparent have many interesting applications in optoelectronic devices such as displays, as well as in defrosting, defogging, gas sensing and point-of-care disposable devices. In recent years, there have been many advances in this area with the advent of next generation transparent conducting electrodes (TCE) based on a wide range of materials such as oxide nanoparticles, CNTs, graphene, metal nanowires, metal meshes and their hybrids. The challenge has been to obtain uniform and stable temperature distribution over large areas, fast heating and cooling rates at low enough input power yet not sacrificing the visible transmittance. This review provides topical coverage of this important research field paying due attention to all the issues mentioned above.

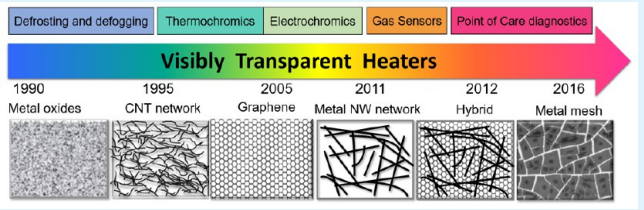

KEYWORDS: *flexible, heating rate, heater, joule heating, transparent, uniform temperature*

1. INTRODUCTION

Tin doped indium oxide (ITO) has been used extensively as a transparent conducting electrode, because it is highly transparent (~90%) and conducting (10 Ω/sq). The amazing properties of ITO have acclaimed wide usage in several optoelectronic devices such as photovoltaic cells, organic light emitting devices (OLEDs), displays, touch screens, smart windows etc.[1] In the modern technology market, there is an increasing trend to make consumer electronics go visibly transparent.[2] However, this cannot be achieved solely using ITO due to its limited availability and increasing price. Moreover, certain applications require flexibility and robustness of electrodes in any given atmosphere, where ITO fails to perform adequately. Alternatives to ITO that are widely studied include metal oxide,[3] graphene[4] and conducting organic (PEDOT:PSS) films[5] as well as networks of carbon nanotubes (CNTs),[6] and metal nanowires.[7] Other alternatives are metal mesh[8] and hybrid nanostructures.[9] These form either a conducting 2D film or a conductive percolative network with reasonable transparency sufficient for optoelectronics.[10] The next generation transparent conductors have broadened the horizon of transparent electronics.[11] The electronic components and devices that need not necessarily be transparent have been made transparent, which include capacitors,[12] tactile strain sensors,[13,14] nanogenerators,[15,16] supercapacitors,[17] photodetectors[18] etc.

A transparent conductor, when made to carry current by applying a few volts, itself acts as a transparent heater. One such optoelectrical appliance is the defrosting and deicing window used typically in LCD panels, vehicles, advertisement boards as well as in display screens of teller machines, avionics etc. Indeed, these constitute a big fraction of the demand of transparent conductors. Transparent heaters tend to outscore hydrophobic coatings for defrosting and anti-icing applications,[19] as the latter exhibit limited mechanical and chemical stability particularly in harsh weather conditions extending over long periods. The transparent heating systems available on the market to defog or deice windshields are in general ITO based heaters.[20] ITOs with conductivity ranging between 1 and 250 Ω/sq and power rating ranging from 0.05 to 20 W/sq.in. are available in the market today. ITO based commercial heaters have very low defect density (<5 μm/sq) over large areas with minimum roughness (R_{rms} < 2 nm).[21] The ITO layer is usually sputtered under vacuum either on flat or on curved glass, because ITO is brittle and cannot be bent or flexed later for use. Typically, ITO films possess modest transmittance (~85%) and good adhesion with the substrate. ITO based heaters are usually laminated with protective layers for ruggedization, mechanical strength and impact resistance. Additionally, optical coatings are applied on the surface of ITO heaters for index matching so as to reduce haze or reflection losses and improve further the transmittance of the heater. Similarly, metallic wire or power line based heaters[22] embedded in the acrylic or glass are used to provide the required transparency in airbus cockpit windows[20] and large display boards.[23,24] However, the thickness of a metal wire being in the range of 10−500 μm obstructs the view and therefore, are not preferred in fine display and controls. This explains the growing demand for transparent heaters in recent years. The valuation of the smart glass market was $1581.4 million in 2013 with 20% growth predicted until 2020.[25] In this

Received: November 15, 2015
Accepted: April 21, 2016
Published: May 13, 2016

DOI: 10.1021/acsami.5b11026
ACS Appl. Mater. Interfaces 2016, 8, 12559−12575

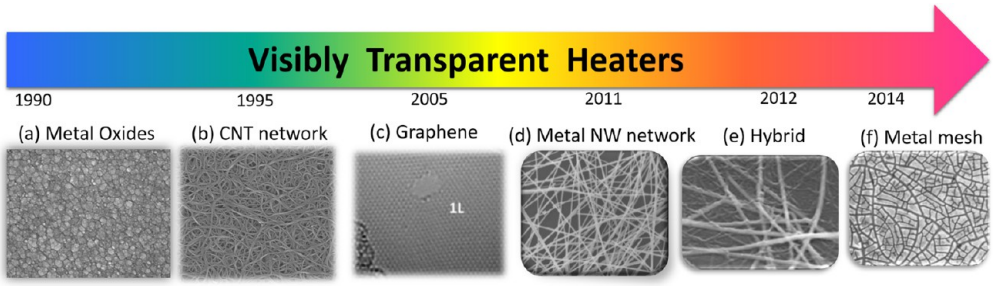

Figure 1. Classification of transparent heaters in chronological order. The year indicates the emergence of the heater using the specified material. (a) Fluorine doped tin oxide. Reprinted with permission from ref 26. Copyright 2014 American Chemical Society. (b) Carbon nanotube network. Reprinted with permission from ref 27 Copyright 2007 Wiley. (c) Graphene. Reprinted with permission from ref 4. Copyright 2015 American Chemical Society. (d) Metal nanowires network. Reprinted with permission from ref 28. Copyright 2015 Springer. (e) Hybrid. Reprinted with permission from ref 29. Copyright 2015 Nature Publishing Group. (f) Metal mesh network. Reprinted with permission from ref 30. Copyright 2015 Wiley.

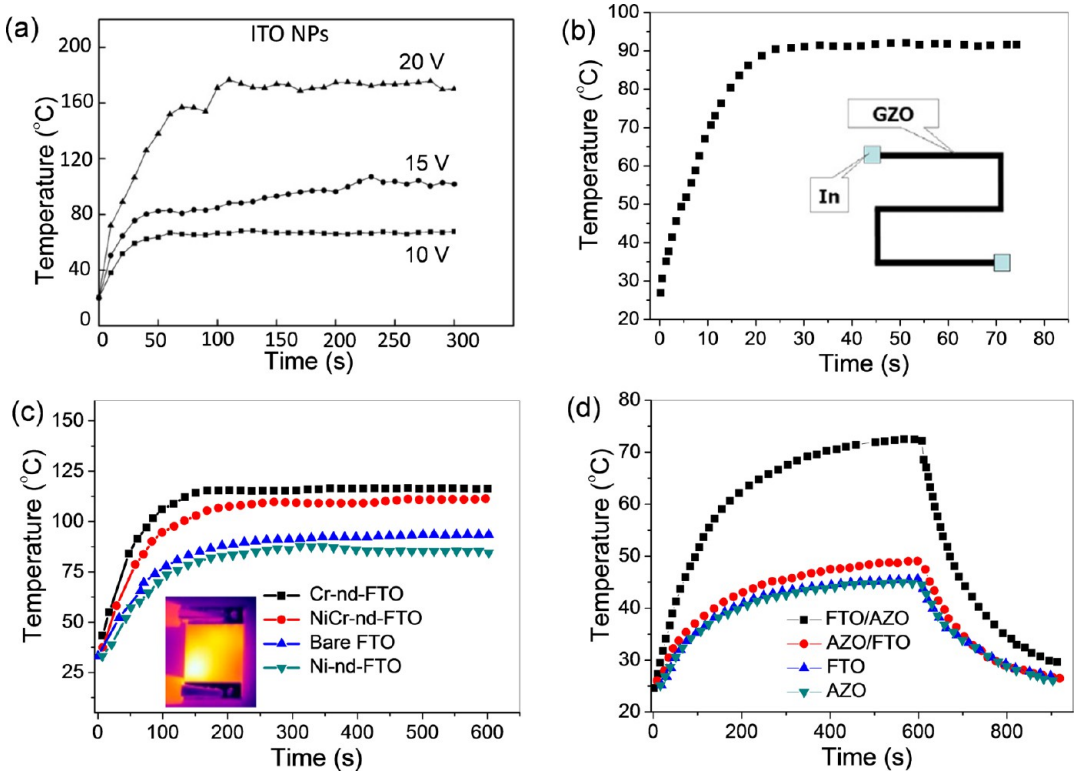

Figure 2. Temperature versus time plot for various metal oxide thin films. (a) ITO. Reprinted with permission from ref 39. Copyright 2010 Elsevier. (b) Ga doped zinc oxide (GZO). Reprinted with permission from ref 43. Copyright 2008 Elsevier. (c) Fluorine doped tin oxide (FTO) and Cr, Ni, Ni−Cr nanodots covered FTO thin films. Reprinted with permission from ref 46. Copyright 2015 American Chemical Society and (d) FTO and aluminum doped zinc oxide (AZO) single layer, double layer structures. Reprinted with permission from ref 26. Copyright 2014 Wiley.

review article, we describe the current status of the field of transparent heaters, highlighting ongoing efforts worldwide in relation to next generation transparent conductors, as categorized chronologically in Figure 1a−f.

The TCEs are ranked by evaluating the figure of merit (FOM) from the ratio of DC and optical conductivities, σ_{OP}/σ_{DC} that relates transmission with sheet resistance (R_S).[31] The electrical and optical properties of these electrodes are optimized by engineering the material design and architecture. Commonly, parameters such as the thickness of the film, network density, area occupied by the material, % of conducting phase, fractal dimension of the network are varied for tuning the transmittance and resistance of a given TCE.[32] The deciding parameter for a heater is its sheet resistance: lower the value, better is its power efficiency. High degree of uniformity of the resistance is another important requirement. For a given applied voltage, the heating rate and the temperature attained, depend on the thermal properties of both the heating element and the substrate, the interface being an additional entity. The heat conduction in the heater film depends upon the thermal conductivity (κ; W/cm/K), which is given by Fourier law as $P/A = -\kappa(dT/dx)$. The convective loss can be expressed using Newton's law of cooling, $q_{conv} = hA(T_S - T_\infty)$ where q_{conv} is input power (W), h is heat transfer coefficient (h is material property), T_S is surface temperature. By presuming that radiative heat power loss is negligible compared to convective heat power loss, the time constant can be obtained from the temperature rise curves according to the

DOI: 10.1021/acsami.5b11026
ACS Appl. Mater. Interfaces 2016, 8, 12559−12575

equation: $T - T_S = \Delta T\ (1 - e^{-t/\tau})$. The increase in temperature of a heater depends on the power generated given as $\Delta T = VI/hA$ where h is the heat transfer coefficient and A is cross-sectional area. The time constant is evaluated using the equation: $\tau = hA/mC$, where h is heat transfer coefficient, m is the specific mass and C is the specific heat capacity of heating element and A is cross-sectional area. Thus, lower the specific heat capacity and lesser the thermal mass, higher would be the temperature for a given input power.[33]

2. CLASSIFICATION OF TRANSPARENT HEATERS

In a transparent heater, a steady state temperature is achieved by controlled joule heating of the transparent conductor and depending on its sheet resistance, the power gets dissipated as heat. The temperature attained by the film is usually detected using a pyrometer, T-type thermocouple or a noncontact IR thermal camera, the latter being advantageous as it provides a macroscopic view of the heat distribution across the heater surface in the form of a surface temperature map. The thermal resolution of an IR camera is usually 10−20 mK and hence suitable in providing temperature distribution over a narrow range of temperature while examining defects as well as hotspots across the active area of a transparent heater. During thermal imaging, the emissivity of the substrate is first calibrated for accurate measurement of temperature. The fabrication of a heater requires good ohmic contacts with the electrode material. The properties that make a transparent conducting electrode ideal as a transparent heater are its low sheet resistance and high thermal stability while not sacrificing the transmittance. Areal uniformity of these properties is also equally essential. A property paid less attention in the literature is the thermal conductivity of a TCE, which plays an important role in applications where temperature variations are involved. For the optimum design of materials, TCEs must qualify certain industrial requirements such as humidity resistance test (>24 h; MIL-C-675), tape-adhesion test (MIL-M-13508), abrasion resistant (MIL-C-675), NaCl solubility resistant (>24 h; MIL-C-675) and temperature stability over a wide range (−54 to +71 °C). For application in displays, industrial standard TCE should possess haze values below 2−3%, as high scattering can cause blurriness.[21] In what follows, we discuss in detail transparent heaters as classified in Figure 1.

2.1. Metal Oxide Thin Film Based Heaters. ITO thin films have traditionally been used for the fabrication of transparent heaters but being brittle, are limited to rigid substrates such as glass.[34] ITO films with thickness of ∼100−300 nm are fabricated by various deposition techniques including chemical vapor deposition (CVD), magnetron sputtering, vacuum evaporation and spray pyrolysis.[35−37] The resistivity of ITO films is typically in the range 10^{-4} Ω·cm with carrier density of $\sim 10^{21}$ cm^{-3},[38] both being inferior to good metals. In the case of solution processed ITO films, the interparticle resistance and surface roughness are usually higher compared to physically deposited films resulting in defects.[39,40] Such high resistivity and low carrier density of ITO results in slow thermal response (Figure 2a), though the temperature uniformity may be appreciable.[39,40] The temperature range that ITO can sustain is rather low, which restricts its use in high temperature applications.[41] Group III elements such as Al and Ga doped in ZnO have been tried out as alternative transparent conducting oxides.[42,43] The Al and Ga metal doping leads to localization of electrons in anisotropic p or d states, thereby influencing the optical and electrical properties of the ZnO film considerably. Kim et al. fabricated Ga doped zinc oxide (GZO) film (90% transmittance) by radio frequency (RF) sputtering at a substrate temperature of 500 °C.[43] A line patterned transparent heater fabricated over 4 cm^2 required voltage as high as 42 V to increase temperature up to 90 °C appreciably, within 22 s. However, Ahn et al.[42] improved the performance of heater dramatically (Figure 2b) by preparing high quality GZO films by pulsed laser technique. Fluorine doped tin oxide (FTO) serves as a substitute for ITO in wide variety of applications including heaters. FTO has high thermal stability as compared to ITO, which is indeed used in applications that require high temperature annealing/heating. It is an n-type semiconductor with a wide bandgap of 3.6 eV and reasonable electrical resistivity, $\sim 10^{-3}$ Ω cm.[44] Fluorine doping can be tuned to improve thermal response of the transparent heater.[45] FTO synthesized on flexible polyethylene terephthalate (PET) substrate has been used for fabrication of a flexible transparent heater.[46] Because FTO film alone exhibited poor thermal characteristics (∼39 °C with 12 V, for example) due to limited conductivity, the film is doped with Ni, Cr and NiCr nanodots for faster thermal response (Figure 2c), which also ensures enhanced distribution of heat via scattered metal nanoparticles.[46] An alternative approach for improving FTO performance is to fabricate hybrid structures with a FTO layer coated on Al doped ZnO (AZO), resulting in larger grain sizes and higher electrical conductivity.[26] In the given instance, the electrical conductivity and carrier mobility of the hybrid structure were increased to 539 $S{\cdot}cm^{-1}$ and 17.6 $cm^2\ V^{-1}\ s^{-1}$ respectively, in relation to single layer AZO (8.55 $cm^2\ V^{-1}\ s^{-1}$ and 204 $S{\cdot}cm^{-1}$) or FTO values (327 $S{\cdot}cm^{-1}$). As a result, FTO/AZO exhibits superior thermal characteristics (Figure 2d).

2.2. Carbon Nanostructures Based Heaters. After an era of conventional ITO electrodes based heaters, the transparent heaters gained renewed attention with the development of transparent and conducting SWNT films.[47] Han and co-workers[27] fabricated the first transparent film heater using SWNTs with transmittance of 79% with R_S of 580 Ω/sq operable at 60 V. The inverse dependence of the steady state temperature with resistance of the SWNT film was examined in this study. As the fabrication and scalability of SWNT films is expensive and process intensive,[47] the transparent heaters were later assembled using MWNT films.[48] Jang and co-workers[49] fabricated heaters using vertically aligned MWNT directly transferred to substrate. However, the fabricated heaters possessed high sheet resistance (∼700 Ω/sq) and moderate transmittance (83%). The length-to-width ratio of MWNTs was tuned to optimize the performance of the heater. The flexibility of individual MWNT sheets was tested by folding and unfolding, while 50 V input voltage was applied. Although CNT derived transparent heaters have shown relatively better performance in terms of low input power and flexibility, they require further development for practical usage.[49,50]

Meanwhile, graphene has attracted tremendous attention as a thin film heating element due to its excellent electrical, optical, mechanical and thermal properties.[51] The high thermal conductivity of graphene (∼5000 W m^{-1} K^{-1}) provides homogeneous temperature distribution and faster heating rates.[47] The optical clarity, low haze, color neutrality, low reflectivity and refractive index matching are additional attributes of graphene. As a successful heater, one would desire to have ∼80% transmittance, which is equivalent to having graphene with few layers of thickness ∼3−5 nm. Sui et al.[52]

DOI: 10.1021/acsami.5b11026
ACS Appl. Mater. Interfaces 2016, 8, 12559−12575

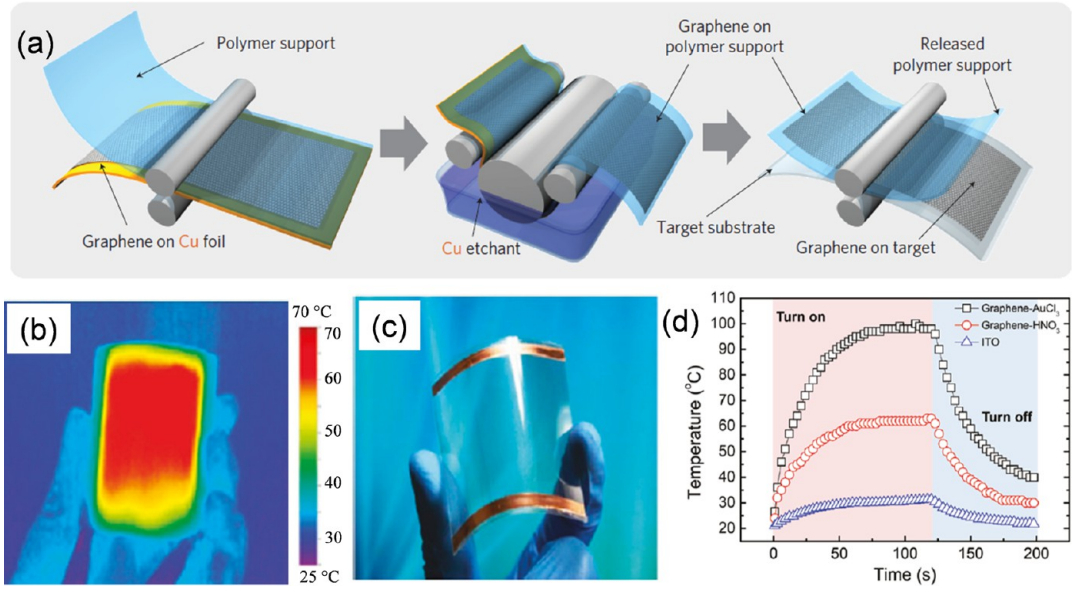

Figure 3. (a) Schematic showing procedure for preparing transparent flexible graphene films with layer-by-layer doping method. Reprinted with permission from ref 53. Copyright 2010 Nature Publishing Group. (b) Thermal image and (c) photograph of graphene based transparent heater in bent positions while an input bias was applied. (d) Temperature rise profiles at 12 V for graphene doped with $AuCl_3$ and HNO_3 in comparison with ITO. Reprinted with permission from ref 51. Copyright 2011 American Chemical Society.

demonstrated a simple, solution-route fabrication of RGO based heater starting with graphene oxide flakes followed by thermal annealing at 800−1000 °C. In the case of graphene film with optimum transmittance of ∼80%, a saturation temperature of 42 °C was achieved by applying 60 V for 2 min. The input voltage is high probably due to the defects, grain boundaries and high contact resistance between the graphene flakes. Moreover, the transparency of the heater is compromised in order to improve the heater performance, which is understandable as graphene film thickness is required to be increased to lower the R_S. The recent advances in graphene production have enabled synthesis of defect-free, high quality graphene by a roll-to-roll CVD process. The CVD system allows synthesis of a monolayer film on a roll of Cu foil as substrate that can be later transferred on other substrates (Figure 3a).[53] Remarkably, these graphene films exhibited low sheet resistance of ∼43 Ω/sq with ∼89% optical transmittance resulting in a low-voltage transparent heater (Figure 3b,c), best known among all carbon based heaters.[51] Doping can be performed to improve the conductivity of graphene films as an alternate to increasing layer thickness. For example, Bae et al.[33] modified graphene film by doping with $AuCl_3$ and reduced R_S up to 66 Ω/sq while retaining a transmittance of ∼90%. This reduced the operational voltage of the heater dramatically without affecting the saturation temperature and the input power. Because graphene has extremely low thermal mass and specific heat capacity as compared to ITO, the temperature attained is higher at the same applied voltage. A higher saturation temperature has been observed for graphene doped with $AuCl_3$ as compared to HNO_3 for the same voltage input of 12 V due to its lowered resistance (Figure 3d).[51] The graphene based heater shows excellent temperature stability even under bent condition with high mechanical strain of 4% unlike ITO films that yield easily at strains above 1%. The extreme flexibility of graphene films is commendable for thin film heating applications that are discussed later.[4,54] However, the grain boundaries in between the graphene layers result in excess joule heating with nonuniform temperature distribution over large areas.[55] Thus, patterning of graphene based inks could result in highly efficient heaters.[55]

2.3. Metal Nanowire Network Based Heaters. The nature of metal nanowire networks is geometrically similar to that of carbon nanotubes as they lie across each other forming cross-bar junctions; however, the junctions are usually less dense in the case of nanowires compared to that of CNTs.[29] As far as material property is concerned, metal nanowires are superior to carbon nanotubes, in terms of electrical conductivity. Among metals, Ag has the highest electrical and thermal conductivities and is thus considered to be one of the best candidates for fabrication of transparent heaters.[56] Ag nanowires (AgNW) can be synthesized through a solution process such as solvo-thermal,[57] polyol[58] and multistep growth methods.[59] For example, in the polyol method developed by Xia and co-workers,[60] $AgNO_3$ is reduced in ethylene glycol in the presence of a nucleating agent and polyvinylpyrrolidone (PVP). The fabricated nanowires are purified and redispersed to form a AgNW ink, which is used for the fabrication of networked film using techniques such as vacuum filtration,[61] rod coating,[62] spray coating[63] and spin coating.[64] The AgNW networks are usually quite conductive (R_S ∼ 10−50 Ω/sq) with high transmittance of ∼90%. The local emissivity and temperature distribution in a metal nanowire network can be modulated by varying the fill fraction of metal wires.[65] The high conductivity of metal nanowires enables higher temperatures at lower input voltages, which is an important feature of a heater. The resistance of the network can be tuned by varying the density of nanowires.[66] In an early effort, Celle et al.[28] fabricated a transparent heater using Ag nanowires (R_S, 33 Ω/sq and transmittance ∼90%), demonstrating joule heating from the homogeneously distributed Ag nanowires. Interestingly, higher heating rates (2 °C/s) were realized as compared to those for CNT networks and graphene.[47] Because the heater temperature is substrate dependent, higher temperatures have been obtained for AgNW networks on poly(ethylene

DOI: 10.1021/acsami.5b11026
ACS Appl. Mater. Interfaces 2016, 8, 12559−12575

naphthalate) compared to glass. The fabrication of a uniformly interconnected Ag nanowire network is crucial to achieve homogeneous temperature distribution in AgNW derived transparent heaters. Kim et al.[67] have addressed this issue by rod coating a dispersion of AgNW with clay platelets (Figure 4a). The fabricated transparent heater showed uniform

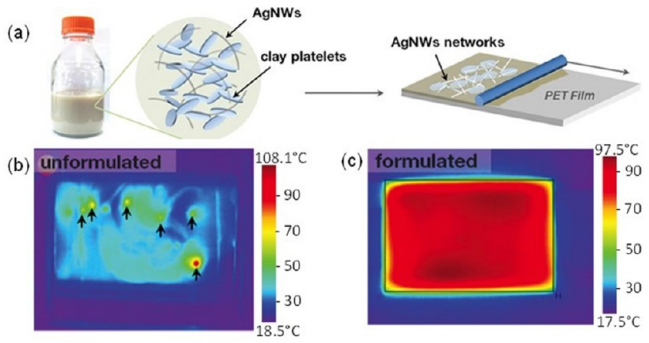

Figure 4. AgNW network (a) AgNWs dispersion in water along with clay platelets. AgNW/clay in the ratio: 2/1 by weight is rod coated on PET substrate resulting in AgNW network. Infrared images of (b) unprocessed AgNW network based heater showing a hot spot due to the self-aggregated nanowires within the networks and (c) a uniform heat distribution for formulated (AgNW and clay platelets) network. Reprinted with permission from ref 67. Copyright 2013 Wiley.

temperature of ~95 °C over a 25 × 20 cm^2 area, whereas that without the clay platelets exhibited several hotspots (Figure 4b) due to self-aggregation of wires, high junction resistance and nonuniformities in the network. It is clear that clay platelets enhance uniformity of nanowire dispersion avoiding self-aggregation resulting in uniform heat distribution (Figure 4c). If the nanowires are sparse, the electrode exhibits higher transmittance but a higher R_S as well. In such networks, the current density in an individual wire is expected to be higher, resulting in high surface temperatures and possible electrical failure.[68,69] Thus, the joule heating ability is limited in the case of metal nanowires due to uneven current densities.

2.4. Metal Mesh Heaters. Conventionally, a metal wire with few micrometer diameter can be physically woven in the form of a mesh with certain spacing resulting in a transparent heater. However, the fabrication process gets harder as the wires become narrower. Thus, the state-of-the-art micro- and nanofabrication techniques have been employed for fabrication of planar metallic patterns for uniform heating without sacrificing transparency. These patch heaters, however, are limited to few square centimeter areas, as lithography processes are expensive. However, simple recipes for prototyping of heaters have been developed using laser printed toner as a template for designing a Ag based heater.[70] The fabricated patterns possessed low R_S, and thus resulting heaters showed excellent thermal response. Although, metal mesh based heaters can be transmitting up to 80%, they are not truly visibly transparent as the grids can be clearly seen with the naked eye. For metal mesh to be visibly transparent, the wire width should be on the order of tens of micrometers or lower. To achieve finer patterns, jet printing[71] and nanosphere lithography[72] methods have been used. However, at widths and spacings comparable to the light wavelength, a periodic mesh can produce optical diffraction effects hindering visibility at certain angles; increasing wire spacing would not help, as it may lead to nonuniform temperatures. Such compelling reasons have led to the fabrication of aperiodic random mesh structures while avoiding expensive lithography processes.[30,73,74] One among these elegant examples is the self-forming crack template method (Figure 5a) for fabrication of mesh electrodes that has been extended to transparent heaters as well.[30] The transparent electrodes fabricated using crack templates exhibited superior performance due to extremely low R_S (~6 Ω/sq) and high T (~86%) values.[30] The uniformity of the fabricated TCE has been tested by joule heating followed by thermal imaging.[75] The transparent heater showed a uniform distribution with a temperature variation of only ~3 °C across a large area

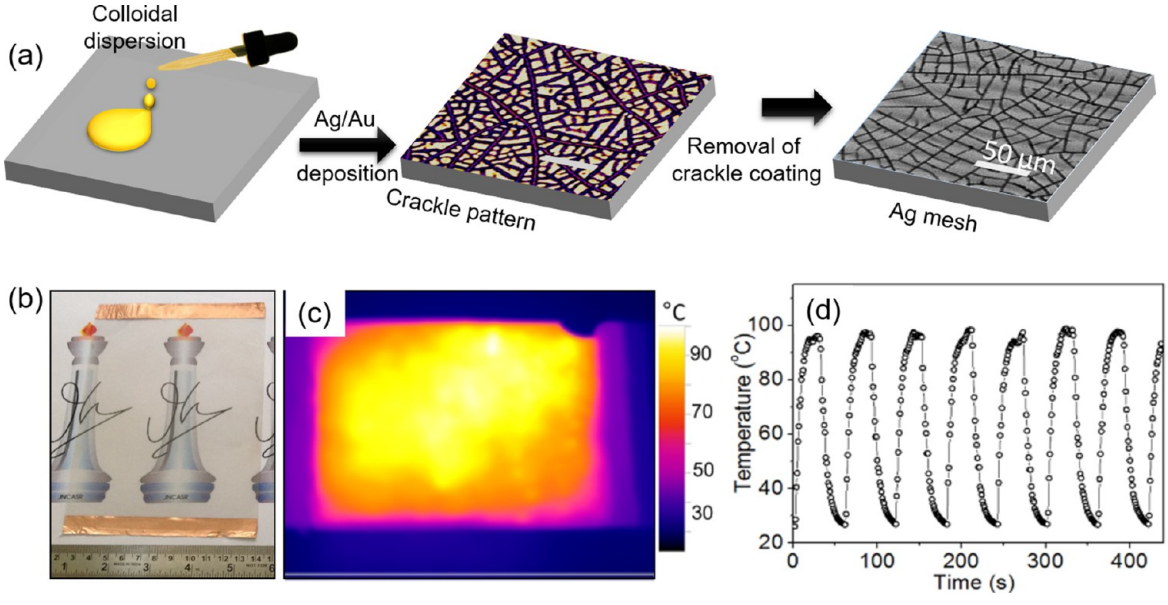

Figure 5. (a) Schematic showing steps for fabrication of crack network based metal mesh. Reprinted with permission from ref 30. Copyright 2014 Wiley. (b) Photograph, (c) thermal image (4 × 2 cm^2) displaying temperature distribution across the surface of transparent heater and (d) heating cycles at an operating voltage of 2.25 V. Reprinted with permission from ref 76. Copyright 2014 American Chemical Society.

DOI: 10.1021/acsami.5b11026
ACS Appl. Mater. Interfaces 2016, 8, 12559−12575

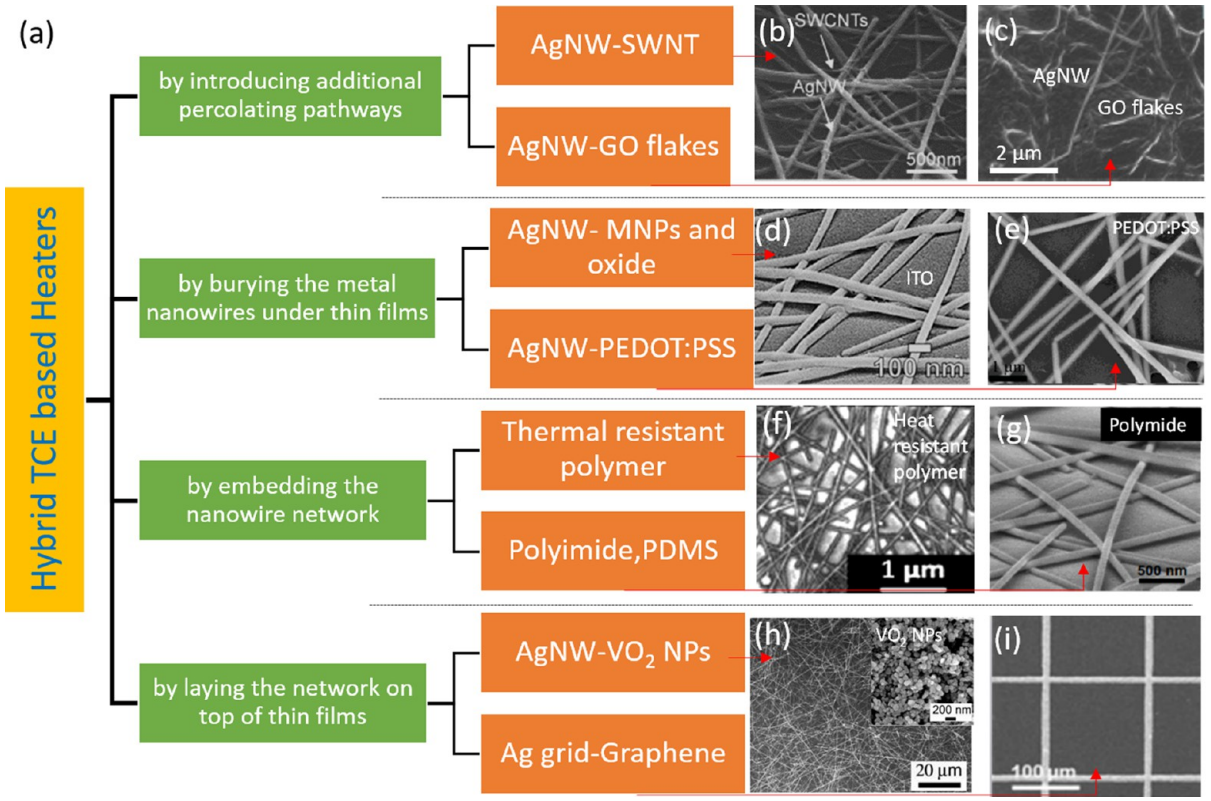

Figure 6. (a) Schematic categorizing the hybrid TCE based heaters (b) SWNTs-AgNW, Reprinted with permission from ref 29. Copyright 2014 Nature Publishing Group. (c) Graphene oxide flakes- AgNW, Reprinted with permission from ref 79. Copyright 2014 Elsevier. (d) ITO-AgNW, Reprinted with permission from ref 81. Copyright 2015 Elsevier. (e) PEDOT:PSS-AgNW, Reprinted with permission from ref 83. Copyright 2014 Wiley. (f) Heat resistant polymer-AgNW, Reprinted with permission from ref 85. Copyright 2014 Wiley. (g) Polyimide-AgNW. Reprinted with permission from ref 86. Copyright 2015 Royal Society of Chemistry. (h) VO_2 nanoparticles (NP)-AgNW, Reprinted with permission from ref 87. Copyright 2014 Royal Society of Chemistry. (i) Graphene-Ag grid, Reprinted with permission from ref 88. Copyright 2015 Royal Society of Chemistry.

importantly without any hotspots (Figure 5b,c). A voltage of ~5 V was sufficient enough to raise the temperature to 93 °C repeatedly over several cycles with good response times (~20 s, Figure 5d).[76] This remarkable performance is attributed to the absence of cross-bar junctions in these networks. Further, metal mesh electrodes fabricated by this approach have been employed in several optoelectronic devices as well.[12,77]

2.5. Hybrid Electrodes Based Heaters. As evident from the above sections, metal oxides and carbon based thin film heaters possess uniform heating; however, due to poor conductivity, the operating voltages are rather high and unrealistic for practical applications.[78] On the other hand, metal network/grid/mesh based heaters although possess high conductivity, require optimized geometry (cell size) for uniform heating. Thus, a combination of metal wire network/mesh and a conductive thin film is a synergistic approach for designing efficient, low power transparent heaters. Such metal wire network based hybrid heaters are fabricated following different approaches: (1) by introducing additional percolating conducting pathways using CNTs or graphene flakes, (2) by burying the wire network under thin films of metal oxides or polymers, (3) by embedding the wire network in insulating polymers or (4) by laying the network on top of thin films. These approaches not only lower the overall R_S of the nanowire networks but also result in homogeneous heating. Few examples of hybrid TCE based heaters based on above-mentioned approaches are shown in Figure 6a. A AgNW/SWNT based hybrid TCE (Figure 6a) is proposed as an electrically robust and scalable method for transparent heaters.[29,66] By the addition of functionalized SWNTs (2.5 wt %) to Ag nanowires in solution, a heater with extremely uniform heating has been realized.[29] Importantly, SWNTs tend to connect with AgNWs conformably leading to higher contact area (see Figure 6b) unlike junctions among the AgNWs. The individual AgNWs are more rigid as compared with SWNTs, and as a result, the contact area varies largely among the AgNW junctions. Moreover, few AgNW junctions may not even be connected in the network as shown in Figure 6b. In spite of a large number of junctions in the network, only a few percolative current paths are possible, whereas in the case of AgNW-SWNT based TCEs, the junctions are engineered to have more contact area leading to lesser junction resistance. These factors lead to uniform heating. Moreover, high thermal conductivity of SWNTs and Fermi level matching between Ag nanowires and modified SWNTs offer additional advantages in addition to optimum heating performance. Zhang et al.[79] reported another strategy where AgNWs were first mixed with small and large flakes of reduced graphene oxide (rSGO, rLGO) and vacuum filtered to obtain a continuous film (Figure 6c). Graphene oxide and AgNW hybrid electrodes formed a continuous film instead of a network. The large graphene oxide flakes spanning over a few micrometers may connect several AgNWs simultaneously, thus enhancing both electrical and thermal energy transport. GO flakes also prevent areal oxidation and melting of AgNWs. The hybrid electrodes were fabricated and annealed at different temperatures (400−700 °C) to optimize the heater perform-

DOI: 10.1021/acsami.5b11026
ACS Appl. Mater. Interfaces 2016, 8, 12559−12575

Table 1. Parameters for Optimum Designing of Materials for Heater Fabrication[a]

features	ITO and oxides	CNTs	graphene	metal nanowires	metal mesh template	hybrid
sheet resistance	****	***	***	**	*	*
transmittance	***	***	****	****	****	***
haze	**	*	*	***	*	**
roughness	**	****	*	***	*	*
cost of processing	**	**	***	*	**	**

[a]The number of asterisks indicate high and low scale.

ance. Interestingly, the rLGO films annealed at 700 °C showed the best joule heating performance at much lower operating voltages. Recently, a hybrid heater of AgNW and graphene oxide film was fabricated by electrostatic interaction between charged layers and AgNW.[80] The heater was transparent up to 90% with a resistance of ∼11 Ω/sq. A response time of ∼100 s to attain ∼60 °C is although not so favorable, it is reasoned to be sufficient for defrosting of windshield in automobiles. Following approach 2, Cheong et al.[81] covered the Ag nanowire network using Ag nanoparticles and sputtered ITO film to confine the heat in the insulating areas and achieve uniform heating (Figure 6d). Similarly, in another example, a Ag mesh heater fabricated using microsphere lithography was obtained as buried under ITO.[82] Poly(3,4-ethylenedioxythiophene) polystyrenesulfonate (PEDOT:PSS) is a conducting polymer that can also be easily spin coated for filling the voids in a nanowire network. Ji et al.[83] coated a PEDOT:PSS layer over a Ag nanowire network film and reduced its R_S to 4 Ω/sq (Figure 6e). The thermal response of the hybrid was found to be substrate thickness dependent. A temperature plateau was obtained within 25 s for a substrate thickness of 0.15 mm, whereas it took more than 300 s for a thickness of 1.1 mm. The thermal resistance (179 °C cm^2 W^{-1}) obtained is significantly high compared to values from ITO and FTO. PEDOT:PSS is highly efficient in redistributing the heat from the hot wires, resulting in uniform temperature distribution.[84] However, use of PEDOT:PSS is avoided for high temperature application due to the possibility of thermal degradation. To address this problem, Li et al.[85] designed heat-resistant polymers that can tolerate high temperatures at low operation voltages. The heat resistant polymer is bonded to the AgNW network as shown in Figure 6f. This AgNW−polymer hybrid could attain a saturation temperature of 230 °C with a low response time. The unique feature of this flexible heater is its long-term working stability as demonstrated by 18 h of continuous operation at 9 V. In another attempt, Lu et al.[86] embedded the AgNWs in polyimide resulting in a hybrid heater (Figure 6g). This resulted in excellent mechanical and thermal stability. In another study, a functional thermo-electrochromic heater was fabricated by coating a layer of VO_2 nanoparticles on Ag nanowires resulting in a hybrid heater (Figure 6h).[87] A large area hybrid heater has been fabricated by printing of Ag mesh over a graphene film (Figure 6i) resulting in R_S of ∼4 Ω/sq and transmittance of 78%.[88] It is clearly observed with statistical analysis that graphene helps in spreading heat from the center of the Ag grid to result in a narrow temperature distribution. Thus, hybrid heaters indeed enhance the thermal response.

The most important characteristics required for the fabrication of a transparent heater are provided in Table 1. As seen in the table, the properties are highly distributed. Among all, metal mesh, metal nanowires and the hybrid materials have high transmittance with low sheet resistance.

The haze value depends on the fill factor, nature of material and the aspect ratio of the nanomaterial under consideration. For example, Ag nanowire networks with a sheet resistance of 45 Ω/sq and 60 nm diameter have shown 12% haze (T = 78%), whereas larger diameter (∼150 nm) has shown a haze value of 28% (T = 72%).[89] Such high haze values are highly undesirable in heaters for displays. There have been many efforts to reduce the haze of TCE either by decreasing the width of the nanowire or by overcoating with another metal. A thin coating of Au over Ag nanowires effectively reduced the haziness by 4%.[90] On the other hand, graphene and nanotube based TCE provide low haze values.[1] Kulkarni and co-workers achieved low haze of 2−3% for Ag mesh (T = 90%) prepared through crackle template technique.[30] A low surface roughness is essential to minimize the probability of hotspots or nonuniform heating. With its extremely low surface roughness (<1 nm), graphene stands out as a clear option. It is evident from its use as a protective coating in hybrid material based heaters.[79] Besides its excellent optical transmittance, electrical conductance and mechanical stability, Ag nanowires possess high peak-to-peak roughness that is more than 2 times the diameter of nanowires. The roughness has been reduced effectively by hot-pressing,[91] or by embedding in polymer matrix.[92] This results in an additional increase in the adhesion of the nanowires to the substrate making these suitable for thin film application. In comparison with Ag nanowires, a hybrid of nanowires with CNT, graphene PEDOT:PSS or oxide films provides more than 50% lower surface roughness.[93,94] For example, after pressing CNT/AgNW-PET at 10 MPa for 30 s, the roughness of the film was reduced while adhesion with substrate increased substantially.[94] In contrast to metal nanowires, metal mesh lie in a single plane on the substrate offering a smooth surface due to its seamless junctions. The overall surface roughness of the metal mesh is found to be >20 nm.[95] Lastly, one also needs to consider the cost of processing for the commercial viability and mass fabrication of the electrothermal heaters. The processing as well as material cost for CNT and graphene is significantly high for obtaining good quality films suitable for heater application. Metal nanowires can easily be solution processed and casted into films in a continuous roll-to-roll process. In contrast, hybrid films may require successive coatings, thus increasing the overall processing cost. The low cost crack templates for a metal mesh network have also demonstrated great potential in terms of scalability and cost.[96]

3. TRANSPARENT HEATER PERFORMANCE

As seen in Section 2, the thermal properties of the heater depend on the electrical and thermal conductivities, specific heat capacity of the active material, substrate type and its thickness. The response time of the heater depends on the additional thermal mass, which is either a substrate or a encapsulant carrying/covering the film heater.[27] These properties directly influence the temperature distribution across the

DOI: 10.1021/acsami.5b11026
ACS Appl. Mater. Interfaces 2016, 8, 12559−12575

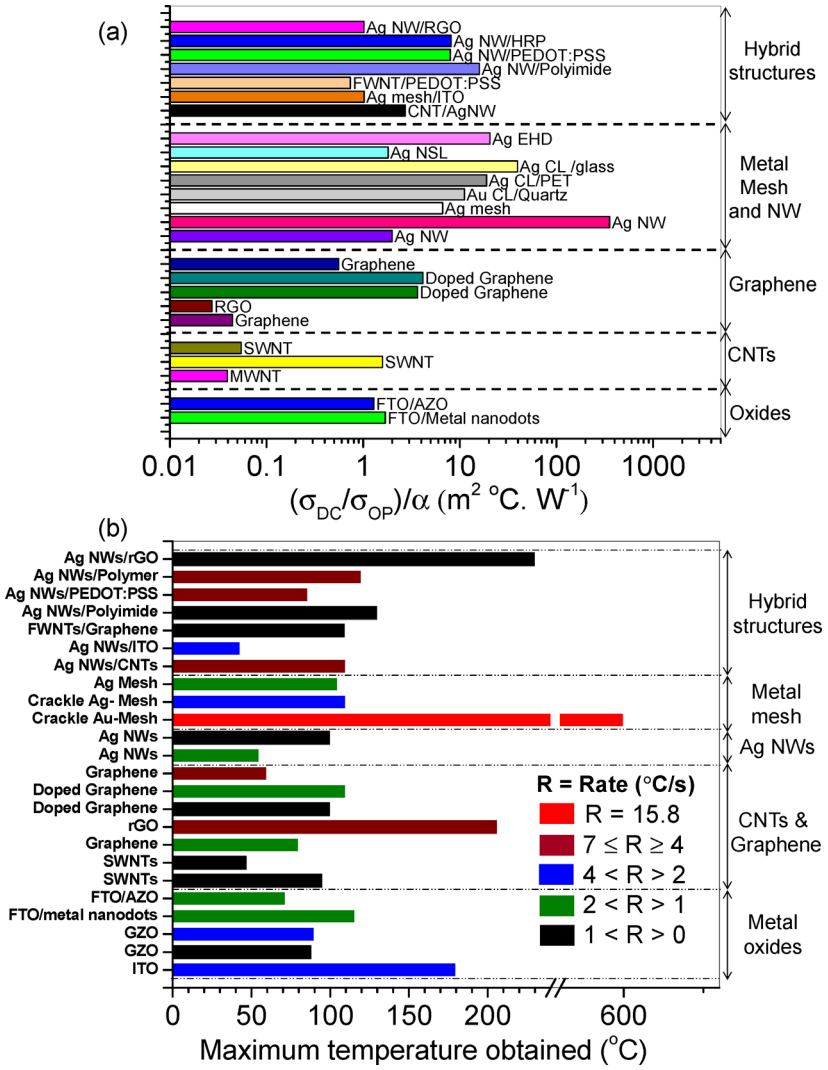

Figure 7. (a) Thermal figure of merit (TFOM) and (b) maximum temperature attained for a specific heating rate calculated using parameters available in literature for various types of transparent heaters.

heater surface. COMSOL Multiphysics modeling can be performed to understand the heat generation, its distribution as well as heat loss mechanisms while designing efficient heaters.[97] The thermal interface resistance between conductor and substrate also influences the heat distribution.[98] Power or heat generated by the heater is given by,[48] $P\ (\text{or}\ \Delta Q) = \frac{V^2}{R\Delta t} = \frac{\Delta Q_{cond}}{\Delta t} + \frac{\Delta Q_{conv}}{\Delta t} + \frac{\Delta Q_{rad}}{\Delta t}$. The radiative heat power loss is expressed by the Stefan−Boltzmann law as $Q_{rad} = \varepsilon\sigma A(T^4 - T_S^4)$, where ε is the surface emissivity, σ is 5.67×10^{-8} W m^{-2} K^{-4}, the Stefan−Boltzmann constant, A is the surface area and T_S the initial surface temperature (in K). Because the emissivity is low for materials with high transparency, the radiative loss is minimum for transparent heaters. The convective heat power loss is given by $Q_{conv} = hA(T - T_S)$ where h is the convective heat transfer coefficient. Bae et al.[33] developed a model for heater that relates time evolution of temperature to the applied voltage or current and heat dissipation as $mC\frac{dT}{dt} = VI - (Q_{conv} - Q_{rad})$ where m, C, T and t are the mass, specific heat capacity, temperature of heater and time respectively whereas Q_{conv} and Q_{rad} are the convective power loss and radiative power loss, respectively.

In the case of nanostructured network films and metallic nanowire mesh electrodes, both convection and radiation are major pathways for heat loss. Because these are interfacial processes, h and ε depend on fill fraction of nanowires (area occupied by nanowires). This aspect has not been paid much attention in the literature and deserves a detailed study. Whereas in the case of graphene film, heat loss is mainly considered to be due to convection because of its low emissivity.

The figure of merit of transparent conductors defined as the ratio of optical and DC conductivities (σ_{OP}/σ_{DC}) as discussed in Section 1, may not hold good for transparent heaters.[99] The heating performance of a heater is usually given by the thermal resistance or by heat transfer coefficient, which are inversely related to each other. Thermal resistance gives information about the heat generation (temperature) with respect to the input power density. In a recent effort by Sorel et al.,[100] the thermal figure of merit (TFOM) was defined for benchmarking the performance of a transparent heater. It is defined as a ratio of conventional FOM and the heat transfer coefficient (α; inverse of thermal resistance),[100] which takes into account the transmission as well. Using this definition, we have calculated TFOM values for various TCE materials from the literature

DOI: 10.1021/acsami.5b11026
ACS Appl. Mater. Interfaces 2016, 8, 12559−12575

Table 2. Performance Comparison in Transparent Heaters[a]

type of heater	synthesis process	substrate	area (cm^2)	voltage (V)	power ($W\ cm^{-2}$)	temp. (°C)	t (s)	R_s ($\Omega\ sq^{-1}$)	T (%)	ref
ITO and other alternating oxides										
ITO NPs	chemical	polyether	NA	50	NA	180	30	2500	>90	40
FTO	physical	PET	5 × 10	12	NA	39	700	253	88	45
GZO	physical	glass	11	12	NA	88	48	NA	>90	42
GZO	physical	glass	2 × 2	42	NA	90	22	NA	90	42
metal/FTO	physical	glass	2.5 × 3.5	12	NA	116	160	26.85	86	46
FTO/AZO	physical	glass	2.5 × 2.5	12	0.275	72	125	36.7	82	26
carbon nanostructures based heaters										
MWNT	physical	PET/glass	0.65 × 0.85	15	0.54[b]	77	NA	699	83	49
SWNT	physical	PET/glass	4 × 4	12	NA	~95	~60	580	79	27
SWNT	physical	glass	1 × 1	60	0.24	47	60	2600	95	98
RGO	chemical	quartz/PI	2 × 1.4	60	2	206	30	641	81	52
doped graphene	physical	PET	4 × 4	12	0.2	100	70	43	89	51
doped graphene	physical	glass	2 × 2	12	0.14	110	200	66	90	33
graphene	physical	PI	2.5 × 2.5		0.02	60	25	520	70	101
metal nanowires and mesh based heaters										
AgNW	chemical	glass/PEN	2.5 × 2.5	7	0.29	55	<200	33	90	28
AgNW	chemical	PET/glass	25 × 20	7	NA	100	<60	10	90	67
Au mesh	physical	quartz	2.5 × 2.5	15	2.6	600	38	5.4	87	95
Ag grid	chemical	PET	1 × 1	0.8	0.35	72	>30	2	60	70
Ag mesh	physical	PET	3.5 × 2.5	NA	0.2	110	20	7	86	76
Ag mesh	physical	quartz	2.5 × 2.5	6	NA	85	150	6	82	75
Ag mesh	physical	glass	2.5 × 2.5	9	0.57	167	200	1	77	102
Ag mesh	chemical	PET	3 × 4	10	0.28	105	NA	20	70	82
Ag grid	chemical	convex lens	~28	5	0.5	105	210	1.49	78	71
hybrid heaters										
CNT and AgNW	chemical	PET	4 × 4	15	NA	110	30	~50	~85	66
AgNW and CNT	chemical	PC	NA	15	NA	150	NA	~20	>90	29
Ag mesh and ITO	chemical	PET	3 × 4	12	NA	43	10	300	88	82
Ag-SWNTs/Graphene/ PEDOT:PSS	chemical	PET	2 × 2	12	0.39	110	<60	93.1	86	78
AgNW/PI	chemical	NA	5 × 5	7	NA	130	<100	25	86	86
AgNW and PEDOT:PSS	chemical	glass/PET	5 × 6	4	0.26	86	<25	4	70	83
AgNW and HR polymer	chemical	NA	2.5 × 4	5	NA	120	40	10	81	85
AgNW and RGO	chemical	quartz	2.5 × 2.5	15	NA	230	<150	27	80	79

[a]NA, not available. [b]Calculated value (AgNW, Ag nanowire; PI, polyimide; PET, polyethyleneterephthalate; HR polymer, heat resistant polymer).

(Figure 7a). In general, metal nanowire and mesh electrodes exhibit the highest TFOM values. The value of TFOM is lower for metal oxides and CNT based networks, which may be attributed to high resistance and greater power requirement for these electrodes.

A transparent heater should attain the desired temperature with low input power. Further, the rate of increase in temperature should be high for applications that require rapid temperature switching. The heating rate depends on the input power, conduction property of the substrate, its thickness as well as the convection and radiation effects, the latter are not so straightforward to deal with. The plot in Figure 7b categorizes heating rate for different types of transparent heaters against the maximum temperature attained by them. As seen in the plot, metal nanowire mesh exhibits exceptional performance because high temperatures are attainable over large areas at a heating rate of 15.8 °C/s. r-GO and hybrid materials based on metal nanowires possess heating rates rates between 0−7 °C/s. Other materials such as CNTs and oxides exhibit heating rates lower than 4 °C/s. The conduction heat losses can be minimized by reducing the thickness of substrate. To avoid convective losses, a direct contact with the substrate is avoided either by creating a vacuum or by suspending the heating element in air. The radiation losses are small for lower temperatures (T < 100 °C), but dominate above 500 °C. For benchmarking the performance, several other key parameters tabulated in Table 2, are also important. On comparison, it is clear that metal meshes exhibit low response times followed by hybrid materials and graphene.[70,95]

4. APPLICATIONS OF TRANSPARENT HEATERS

For transparent heaters to be applicable in daily life applications, they need to possess good mechanical flexibility, robustness and operational stability when integrated into different optoelectronic devices.[98] CNTs, graphene and metal mesh based heaters have been demonstrated to possess high flexibility as compared to traditional ITO electrodes based heaters.[48,52,56,103] However, a transparent heater finds applications such as in cars and airplane window panels where flexible transparent heaters may not conform well to the curved surfaces. Recently, stretchable heaters that can conform to the curvilinear surfaces have been developed using metal nanowire networks.[104] Obviously, the fabrication method should be adaptable to curved objects, so that the heat loss involving the host polymer substrate may be avoided. A TCE fabricated on a

DOI: 10.1021/acsami.5b11026
ACS Appl. Mater. Interfaces 2016, 8, 12559−12575

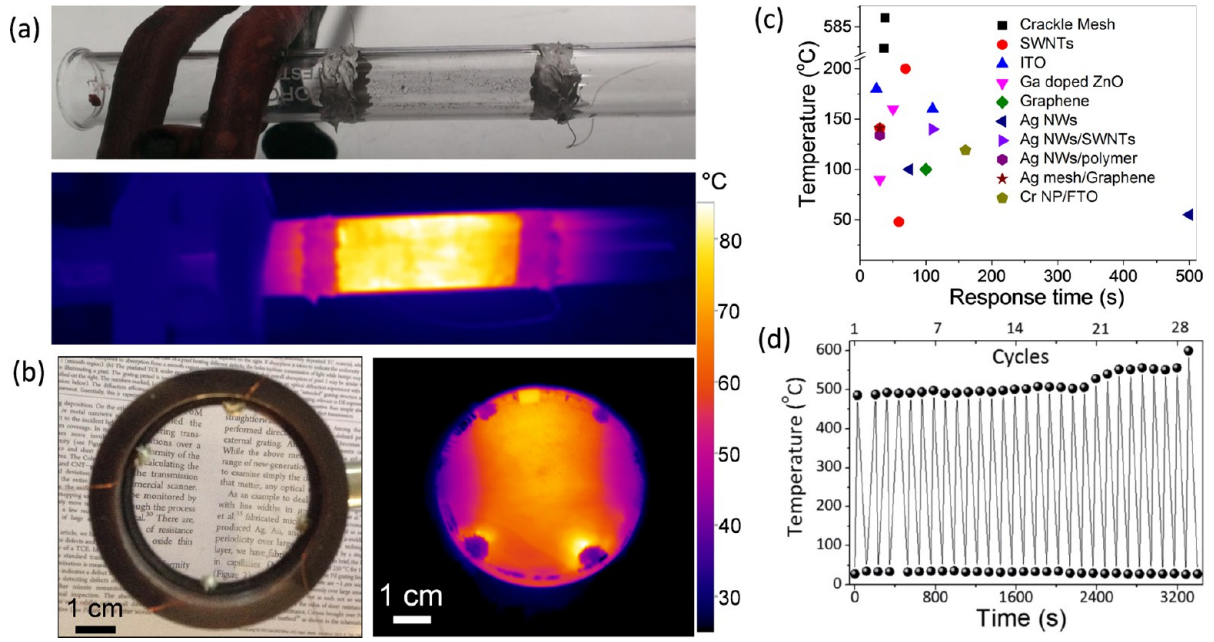

Figure 8. Different attributes of metal mesh heaters fabricated by crackle lithography technique. (a) Ag mesh on outer surface of quartz tube and (b) over convex lens along with the corresponding thermal images. The letters behind the convex lens are seen magnified with clarity. Reprinted with permission from ref 76. Copyright 2014 American Chemical Society. (c) Comparison plot of maximum temperature achieved versus response time for different heaters. Reprinted with permission from ref 95. Copyright 2014 Royal Society of Chemistry. (d) Stability and recyclability of a high temperature heater tested at a switching voltage of 0 and 12 V. The heater was stable even after 30 cycles. Reprinted with permission from ref 95. Copyright 2014 Royal Society of Chemistry.

Table 3. Comparison of TCE and Defrosting Parameters for Various Materials from Literature[a]

	TCE parameters							
material	T (%)	R_S (Ω sq^{-1})	temp. (°C)	area (cm^2)	frost conditions	voltage (V)	time (s)	ref
ITO NPs	>90	2500	70	NA	dry ice	50	10	40
ITO NPs	>90	633	163	NA	dry ice	20	10	39
SWNT	91	1190	120	2.5 × 2.5	freezer	12	60	27
MWNT	85	699	37	2.5 × 2.1	freezer	10	18	49
MWNT	51	172	42	NA	freezer	10	10	107
RGO	45	5370	NA	NA	freezer	10	80	54
RGO	81	6079	45	2 × 1.4	freezer	60	120	52
graphene	85	750	55	NA	freezer	30	30	33
AgNW	92	11	NA	2.5 × 2.5	freezer	10	40	56
AgNW	>90	50	70	NA	freezer	12	60	67
patterned Ag	60−80	2	100	6 × 6	freezer	0.8	>30	70
Ag mesh	77	1	170	10 × 8	−60 °C, LN_2 vapors	8.5	120	102
RGO/AgNW	80	27	150	2.5 × 2.5	freezer	10	40	79
PEDOT:PSS-AgNW	70	4	90	5 × 6	freezer	6	40	83
Ag NWs-PI	86	25	110	5 × 5	freezer	6	60	86
HR polymer-AgNW	86	25	115	7.5 × 7.5	dry ice	9	20	85
ITO-Ag mesh	88	300	43	3 × 4	freezer	12	20	82

[a]NA, not available.

curved surface may be good enough to be a TCE, but may not necessarily work as an efficient transparent heater. TCE is required to be completely defect-free not only to ensure uniform heating but also to have long-term thermal stability, which become critical especially on curved surfaces. The first 3D transparent heater was reported using Ag metal mesh produced by crackle lithography directly on test tube (Figure 8a) and convex lens (Figure 8b) surfaces.[76] In a later work, a jet printing method has been demonstrated to produce 3D heaters by fabricating a periodic mesh (7 μm width and 100 μm pitch) on curved glass with transmittance of 83.5%.[71]

For a heater to attain high temperature, the heating element should stand high current density. CNT based films have shown a great potential as high temperature heaters, but are made so thick that transparency gets compromised.[105] This brings out the trade-off issue between transmittance and resistance and in turn, the saturation temperature for a high temperature transparent heater. In fact, fabrication of a high temperature transparent heater operable at moderate input power is indeed challenging. Among conventional oxides, FTO, although known for its high thermal stability (up to 500 °C) requires high input power relatively to metal films. This may be

DOI: 10.1021/acsami.5b11026
ACS Appl. Mater. Interfaces 2016, 8, 12559−12575

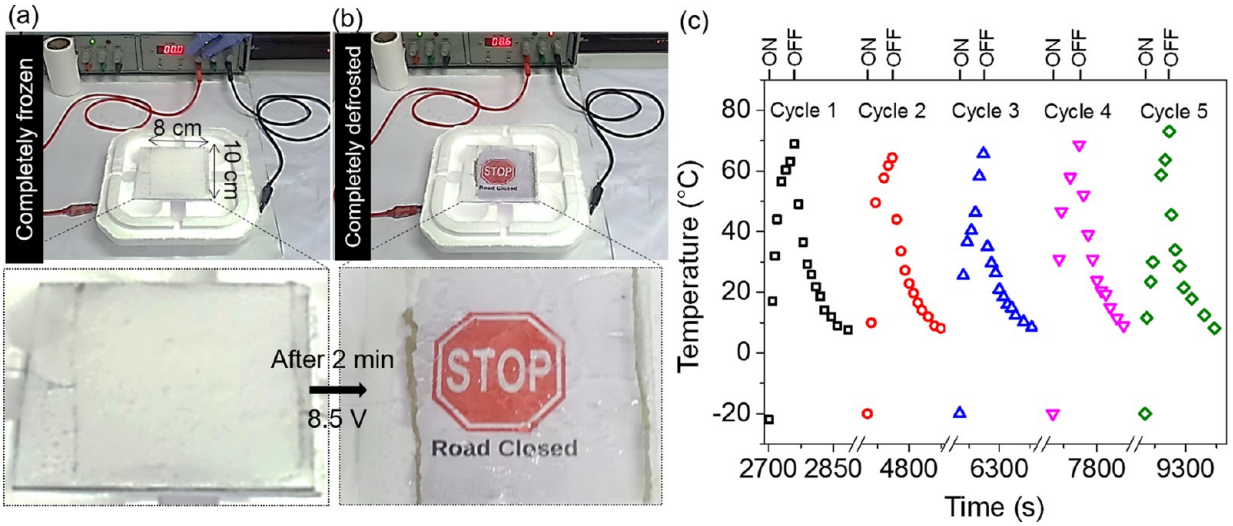

Figure 9. Demonstration of large area defrosting application with Ag mesh/glass. (a) Frost was allowed to form over transparent heater by keeping it over liquid nitrogen (LN_2) container. (b) Frost was removed by applying 8.5 V for 2 min, allowing the visibility of bottom display (refer bottom images of panels a and b). (c) Performance of frost and defrost cycles. V_{ON} refers to 3 V. The heater remains stable even after 7 cycles, which is remarkable aspect of this heater. Reprinted with permission from ref 102. Copyright 2014 Royal Society of Chemistry.

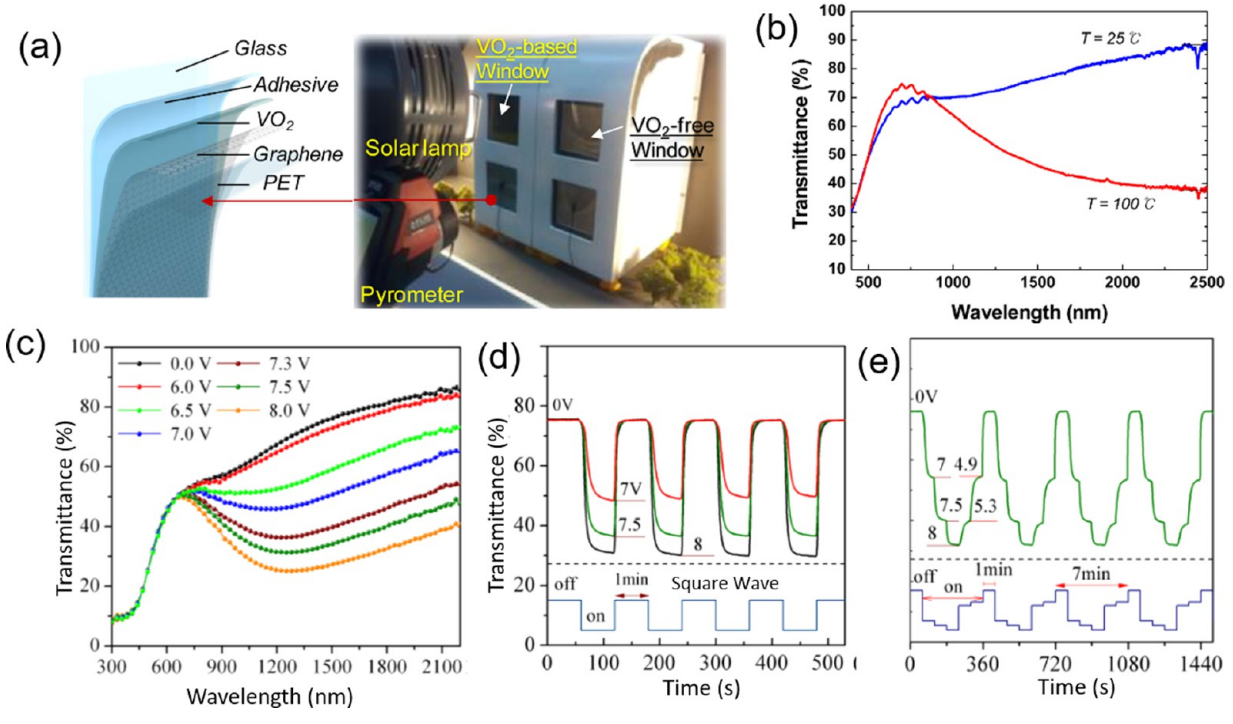

Figure 10. (a) Thermochromic window of the graphene-supported VO_2 film along with photograph of model house. (b) Transmission spectra of the VO_2/graphene/PET film taken at temperatures of 25 and 100 °C. Reprinted with permission from ref 111. Copyright 2013 American Chemical Society. (c) Transmission spectra of VO_2/AgNW based device at different applied voltages. Infrared response at 1.5 μm of the VO_2/AgNW film upon input pulse voltage with (d) square wave and (e) square wave with step variations. Reprinted with permission from ref 87. Copyright 2014 Royal Society of Chemistry.

attributed to the high thermal mass of FTO arising due to thicker films (500 nm) and high specific heat capacity, which increase dissipation.[44] A high-temperature, transparent heater working at 600 °C was fabricated using Au wire mesh while retaining transmittance above 90% (Figure 8c).[95] The exceptional heating performance is attributed to seamless and fully interconnected Au wires (width ~2 μm, thickness of ~220 nm) with very low sheet resistance (3.1 Ω/sq). A remarkable feature of this heater is the improvement in its sheet resistance and transmittance upon operation, due to annealing of Au wires, which was also reflected in increase in its saturation temperature upon cycling (Figure 8d).

4.1. Defrosting Windows. Defrosting using transparent heaters is one of its most common applications. Frost formation and icing cause serious safety issues in cold countries,[22,106] where transparent heaters play a vital role. An important requirement in defrosting application is the ability to heat uniformly with a low response time. The transparent

DOI: 10.1021/acsami.5b11026
ACS Appl. Mater. Interfaces 2016, 8, 12559−12575

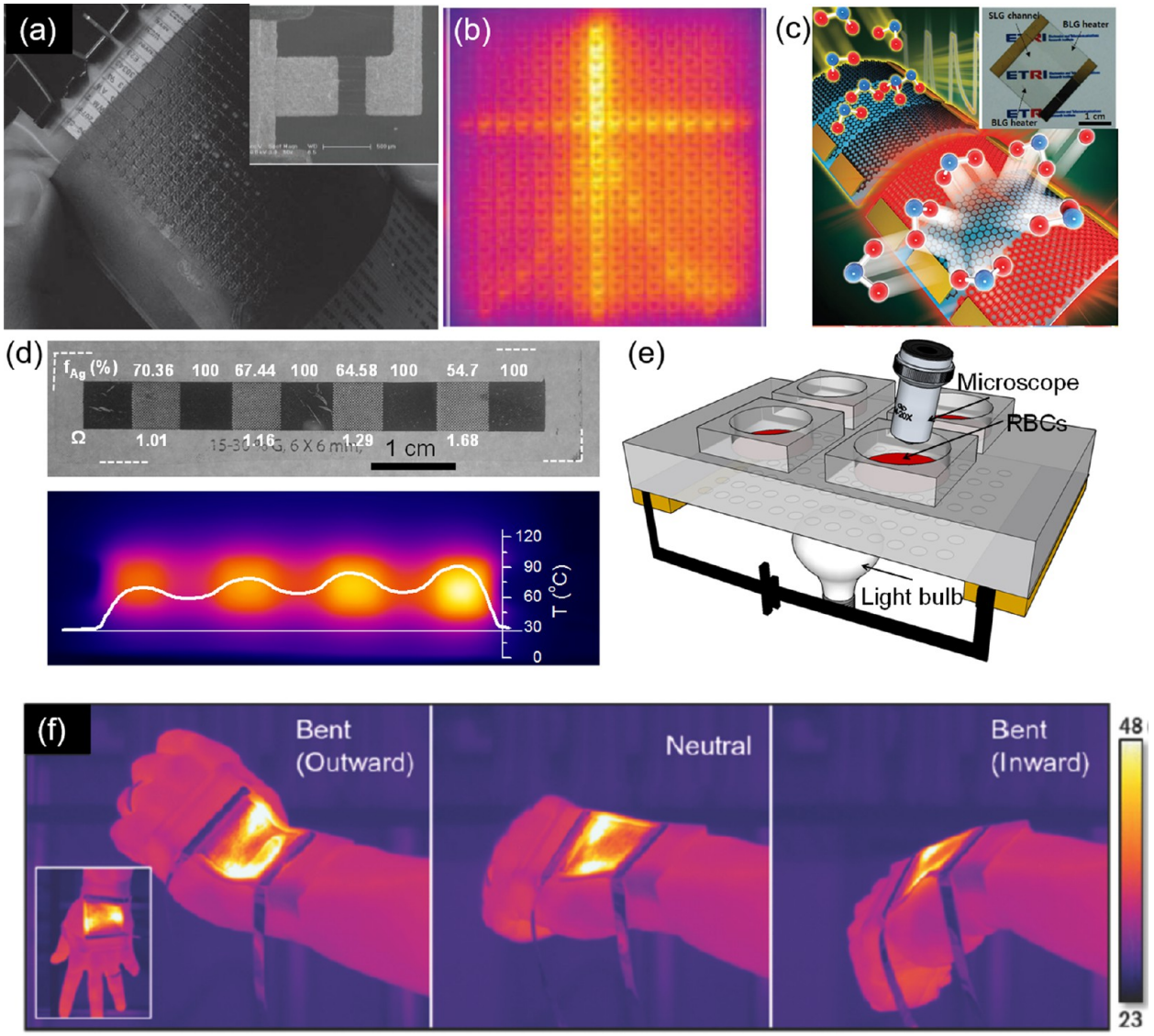

Figure 11. Other applications of transparent heaters: (a) Curved thermochromic display with CNT-film microheater array on PET with inset showing SEM image of the micro-CNT-film heating element. (b) Infrared image of a Chinese character displayed by the CNT-film microheater array. Reprinted with permission from ref 117. Copyright 2011 Wiley. (c) Transparent graphene based gas sensor integrated with graphene heater. Reprinted with permission from refs 119, 123. Copyright 2014 Wiley. (d) Photograph and thermal image of addressable heater array. These heating platforms were utilized to study the thermochromic effect using fluorescent R6G dye. (e) Microscopic stage for thermal imaging of red blood cells. The heater platform was also utilized as a microscopic substrate for carrying out chemical reactions in situ under an optical microscope. Reprinted with permission from ref 120. Copyright 2015 Wiley. (f) Thermal images of stretchable transparent heater affixed on wrist in different positions. Reprinted with permission from ref 104. Copyright 2015 Wiley.

heaters for defrosting are usually studied by creating the frost either by placing the heater inside a refrigerator as done in the case of carbon materials (CNTs,[27] graphene,[33] RGO[52]), metal nanowires[67] and hybrid materials[79] or by placing ITO films[39,40] on top of dry ice blocks. In the above examples, besides the nominal frost load, defrosting phenomenon was tested with small electrode area of ∼1 $in.^2$ with relatively higher voltages (Table 3). In a recent report on a Ag mesh heater, extreme cold conditions have been mimicked with a thick frost layer (Figure 9a) that disappeared instantly after applying a nominal power (Figure 9b).[102] The exceptional performance of the heater was attributed to its highly conducting network (∼1 Ω/sq). Bae et al.[33] elucidated heat transfer mechanism for defogging using graphene and Cr films. Table 3 shows the defrosting windows fabricated using different electrode materials. It would be difficult to compare the performance of various heaters for defrosting applications until their operational stability can be examined. In the example given in Figure 9c, the reliability of the Ag mesh heater for defrosting application has been studied by performing several frost cycles, allowing a thick frost layer to form after each cycle.[102]

4.2. Thermochromic Devices for Smart Windows. Out of the total world's energy consumption, 30−40% is consumed in heating or cooling indoors of buildings and vehicles. If the windows can be designed to be efficient, the energy consumption can be brought down while maintaining the thermal comforts.[108] In winters, the transparent windows can be heated to reduce the cooling load.[109] Simultaneously, thermochromic materials can be incorporated in transparent heaters to enable smart windows that can regulate optical

DOI: 10.1021/acsami.5b11026
ACS Appl. Mater. Interfaces 2016, 8, 12559−12575

transmission when triggered by temperature. These devices contain an active thermochromic material coated on a transparent heater. Among many inorganic and organic thermochromic materials, W doped VO_2 has become popular as it undergoes reversible phase transition from IR transparent to reflective, close to ambient temperatures upon gentle heating.[110]

Yang and co-workers fabricated a thermochromic smart window using VO_2 nanoparticles integrated with graphene as a smart window material, as shown in Figure 10a.[111] As the temperature of hybrid window was raised to 100 °C, there was a decrease in the IR transmission and *vice a versa* (Figure 10b). Ag nanowires based heaters have also been integrated with solution processed VO_2 nanoparticle film for realizing a thermochromic device.[87] It showed a 50% change in its optical transmission in the near IR region as the temperature was raised from 25 to 100 °C, demonstrating an excellent infrared modulation ability (Figure 10c). In these devices, fast switching of temperature is an important attribute (Figure 10d,e). There are several other transparent heaters that have been tested in combination with thermochromic dyes. For example, Kim et al.[66] used a transparent hybrid heater (CNTs and AgNW) wrapped around the beaker containing a thermochromic dye for tuning its color while applying different voltages to the heater. Indeed, the dye changed color, which was aesthetically appealing. In other report, highly transparent Ag nanowire based TCE was used to fabricate a thermochromic device, which switched color around 45 °C.[28]

4.3. Pixelated Heating Display. Development of heaters for MEMs, biochips, artificial skin, point of care devices require patterning of heaters to fit them as pixelated microheaters in integrated devices.[112−115] It is highly desirable to make transparent disposable heaters for bioclinical studies as well.[116] Microheaters are small high power thermal heaters with precise control over both temperature and pixels to be heated.[117] Flexible and transparent graphene based microheaters with high sheet resistance of ∼kΩ have been designed to be effectively powered by a triboelectric nanogenerator of high internal resistance.[118] Liu et al. produced thermochromic displays by patterning a CNT film in a 16 × 16 microheater array by lithographic patterning (Figure 11a).[117] The microheating element consisted of 2 × 2 mm aligned CNT film each with a resistance ∼400 Ω and several such microheaters were assembled at a spacing of 3 mm (Figure 11b). In a recent work, Choi and co-workers[119] micropatterned graphene single and double layers for integrating a transparent heater for a transparent NO_2 gas sensor (Figure 11c). The hybrid structure enables complete utilization of graphene functionalities resulting in commendable sensing performance (12% sensitivity for 1 ppm of NO_2 gas) even under a bending strain of 1.4%. The self-integrated heater led to complete and rapid recovery (∼11 s) with reproducible sensing cycles. In another work by Walia et al., a semitransparent and flexible heater array in the form of a thermal library was created for combinatorial studies (Figure 11d).[120] The heating zones connected in series possess different resistances due to varying metal fill factor. As the library was powered through a laptop USB, the different zones attained different temperatures depending on local resistance but all at once. This shows the efficacy of the integrated mesh type heaters (Figure 11e).[120] The transparent heater is potentially a low cost, disposable, point of care platform for transmission microscopic studies as demonstrated by imaging of blood cells, subjected to thermal stress. Such heaters may also find applications where combinatorial studies involving temperature variations are crucial. In another example, a thermochromic library was created using a thin film of VO_2 with varying Nb doping to reduce the critical transition temperature.[121] Transparent heaters can also find applications as heating pads on a table during computerized tomography (CT) and X-ray testing as demonstrated using a Ag mesh electrode.[82] The fabrication of heaters can also be carried out on nontransparent insulating surfaces such as prewoven textiles. For example, Hsu et al.[122] demonstrated fabrication of transparent heaters in the form of wearable heaters for personal thermal management. The flexible and stretchable transparent heaters made of partially embedded Ag nanowires have been demonstrated to operate at 60 °C at 60% strain. This could serve as an ideal platform for fabrication of wearable electronics devices (Figure 11f). The mass production methods need to be developed further for commercialization of these energy efficient smart heating platforms.

5. CLOSING REMARKS AND FUTURE PERSPECTIVE

This review has covered important aspects and recent developments related to transparent joule heaters. Innovative approaches to realize transparent heaters from novel nanomaterials such as metal oxide nanoparticles, CNTs, graphene, metal nanowires and metal meshes, have been described. Aspects related to the performance of heaters are discussed detailing on achievable heating rates and thermal figure of merit values for the literature examples. The biggest challenge facing the development of invisible heaters is the requirement of low resistance without compromising the transmittance, a trade-off issue common to all transparent conductors. A sheet resistance in the range ∼2−10 Ω/sq, transmittance >80%, haze <10% is considered desirable along with a neutral color. Among the examples discussed here, heaters based on metal nanowire networks and metal meshes appear to be most promising.

The review emphasizes new methods developed to fabricate flexible, 3D conformable electrodes while projecting them for futuristic applications. There is also some discussion on transparent heaters that go beyond conventional temperatures meant for use in specialized applications. The durability and mechanical stability of heaters is an important aspect, and thus flexibility of heaters as well as ability to fabricate the heaters on curved surfaces are being given much attention. Operational stability of heaters is yet another concern. Applications used in military require transparent heaters to sustain harsh environmental conditions, and thus it is important to test the heaters under extreme heating conditions. From the material perspective, optically clear protective coatings may be developed for such purposes. Issues related to performance such as thermal heat distribution, uniformity and stability of the transparent heaters have been discussed in relation to the thermal properties of the active material. However, a clear understanding of the thermal resistance between the substrate and the heating element is still lacking in the literature. The issues concerning hotspots and defective heating have been related to a poor adhesion of the heating element with the substrate resulting in nonefficient heat transfer and correspondingly, nonuniform temperatures. To a large extent, the heating performance is decided by the substrate properties. A self-standing heater without any support substrate can result in a better heating performance in terms of response time, applied power and temperature attained. The ultrathin and thermally

DOI: 10.1021/acsami.5b11026
ACS Appl. Mater. Interfaces 2016, 8, 12559−12575

conducting materials such as mica can be preferably used in cases where substrate is indispensable.

The efforts being made in the literature toward possible commercialization of next generation transparent heaters is also presented. Graphene has immense potential as an electrothermal heater owing to its high thermal conductivity and low thermal mass even at higher temperatures, as evident by its recent commercialization by XEFRO.[124] For a high performance heater, it is usually fabricated only over limited area that may be useful in certain applications such as sensors and heating films. However, real world applications such as defrosting and defogging require a heater almost the size of a window. This demands development of inexpensive fabrication methods for transparent materials that can be applied as heaters. In large area films, occurrence of defects is common due to nonuniformities from manufacturing and this can result in failure of the heaters. Innovative hybrid materials and hierarchical structures are to be designed in the future addressing these considerations. There exist enormous future opportunities for large area heaters with integrated functionality, which include solar modulation windows, wearable devices and low cost point-of-care chips for combinatorial study.

AUTHOR INFORMATION

Corresponding Authors

*Email: Dr. Ritu Gupta (ritu@iitj.ac.in).
*Email: Prof. Giridhar U. Kulkarni (guk@cens.res.in).

Author Contributions

The paper was written through contributions of all authors. All authors have given approval to the final version of the paper.

Notes

The authors declare no competing financial interest.
[⊥]On lien from JNCASR, Bangalore, India.

ACKNOWLEDGMENTS

Authors thank Prof. C. N. R. Rao for his encouragement. The financial support from DST, India is gratefully acknowledged. R.G. acknowledges Department of Chemistry, IIT Jodhpur for the financial support. K.D.M.R. acknowledges CeNS, Bangalore for a postdoctoral fellowship. S.K. acknowledges DST-INSPIRE for fellowship.

REFERENCES

(1) Hecht, D. S.; Hu, L.; Irvin, G. Emerging Transparent Electrodes Based on Thin Films of Carbon Nanotubes, Graphene, and Metallic Nanostructures. *Adv. Mater.* **2011**, *23*, 1482−1513.

(2) Thiriat, S. Toaster Having Transparent Heating Walls. Patent US6341554 B2, January 29, 2002.

(3) Pasquarelli, R. M.; Ginley, D. S.; O'Hayre, R. Solution Processing of Transparent Conductors: From Flask to Film. *Chem. Soc. Rev.* **2011**, *40*, 5406−5441.

(4) Ferrari, A. C.; Bonaccorso, F.; Fal'ko, V.; Novoselov, K. S.; Roche, S.; Boggild, P.; Borini, S.; Koppens, F. H.; Palermo, V.; Pugno, N.; Garrido, J. A.; Sordan, R.; Bianco, A.; Ballerini, L.; Prato, M.; Lidorikis, E.; Kivioja, J.; Marinelli, C.; Ryhanen, T.; Morpurgo, A.; Coleman, J. N.; Nicolosi, V.; Colombo, L.; Fert, A.; Garcia-Hernandez, M.; Bachtold, A.; Schneider, G. F.; Guinea, F.; Dekker, C.; Barbone, M.; Sun, Z.; Galiotis, C.; Grigorenko, A. N.; Konstantatos, G.; Kis, A.; Katsnelson, M.; Vandersypen, L.; Loiseau, A.; Morandi, V.; Neumaier, D.; Treossi, E.; Pellegrini, V.; Polini, M.; Tredicucci, A.; Williams, G. M.; Hee Hong, B.; Ahn, J. H.; Min Kim, J.; Zirath, H.; van Wees, B. J.; van der Zant, H.; Occhipinti, L.; Di Matteo, A.; Kinloch, I. A.; Seyller, T.; Quesnel, E.; Feng, X.; Teo, K.; Rupesinghe, N.; Hakonen, P.; Neil, S. R.; Tannock, Q.; Lofwander, T.; Kinaret, J. Science and Technology Roadmap for Graphene, Related Two-Dimensional Crystals, and Hybrid Systems. *Nanoscale* **2015**, *7*, 4598−4810.

(5) Angmo, D.; Krebs, F. C. Flexible ITO-Free Polymer Solar Cells. *J. Appl. Polym. Sci.* **2013**, *129*, 1−14.

(6) Du, J.; Pei, S.; Ma, L.; Cheng, H. M. Carbon Nanotube and Graphene Based Transparent Conductive Films for Optoelectronic Devices. *Adv. Mater.* **2014**, *26*, 1958−1991.

(7) Ye, S.; Rathmell, A. R.; Chen, Z.; Stewart, I. E.; Wiley, B. J. Metal Nanowire Networks: The Next Generation of Transparent Conductors. *Adv. Mater.* **2014**, *26*, 6670−6687.

(8) Guo, C. F.; Ren, Z. Flexible Transparent Conductors Based on Metal Nanowire Networks. *Mater. Today* **2015**, *18*, 143−154.

(9) Hu, L.; Wu, H.; Cui, Y. Metal Nanogrids, Nanowires, and Nanofibers for Transparent Electrodes. *MRS Bull.* **2011**, *36*, 760−765.

(10) Kulkarni, G. U.; Kiruthika, S.; Gupta, R.; Rao, K. D. M. Towards Low Cost Materials and Methods for Transparent Electrodes. *Curr. Opin. Chem. Eng.* **2015**, *8*, 60−68.

(11) Ellmer, K. Past Achievements and Future Challenges in the Development of Optically Transparent Electrodes. *Nat. Photonics* **2012**, *6*, 809−817.

(12) Gupta, R.; Rao, K. D. M.; Kulkarni, G. U. Transparent and Flexible Capacitor Fabricated Using a Metal Wire Network as a Transparent Conducting Electrode. *RSC Adv.* **2014**, *4*, 31108−31112.

(13) Zhu, G.; Yang, W. Q.; Zhang, T.; Jing, Q.; Chen, J.; Zhou, Y. S.; Bai, P.; Wang, Z. L. Self-Powered, Ultrasensitive, Flexible Tactile Sensors Based on Contact Electrification. *Nano Lett.* **2014**, *14*, 3208−3213.

(14) Gutruf, P.; M Shah, C.; Walia, S.; Nili, H.; S Zoolfakar, A.; Karnutsch, C.; Kalantar-zadeh, K.; Sriram, S.; Bhaskaran, M. Transparent Functional Oxide Stretchable Electronics: Micro-Tectonics Enabled High Strain Electrodes. *NPG Asia Mater.* **2013**, *5*, e62.

(15) Lin, L.; Hu, Y.; Xu, C.; Zhang, Y.; Zhang, R.; Wen, X.; Lin Wang, Z. Transparent Flexible Nanogenerator as Self-Powered Sensor for Transportation Monitoring. *Nano Energy* **2013**, *2*, 75−81.

(16) Kim, S.; Gupta, M. K.; Lee, K. Y.; Sohn, A.; Kim, T. Y.; Shin, K. S.; Kim, D.; Kim, S. K.; Lee, K. H.; Shin, H. J.; Kim, D. W.; Kim, S. W. Transparent Flexible Graphene Triboelectric Nanogenerators. *Adv. Mater.* **2014**, *26*, 3918−3925.

(17) Jung, H. Y.; Karimi, M. B.; Hahm, M. G.; Ajayan, P. M.; Jung, Y. J. Transparent, Flexible Supercapacitors from Nano-Engineered Carbon Films. *Sci. Rep.* **2012**, *2*, 773.

(18) Liu, Z.; Parvez, K.; Li, R.; Dong, R.; Feng, X.; Mullen, K. Transparent Conductive Electrodes from Graphene/PEDOT:PSS Hybrid Inks for Ultrathin Organic Photodetectors. *Adv. Mater.* **2015**, *27*, 669−75.

(19) Lv, J. Y.; Song, Y. L.; Jiang, L.; Wang, J. J. Bio-Inspired Strategies for Anti-Icing. *ACS Nano* **2014**, *8*, 3152−3169.

(20) http://www.saint-gobain-sully.com/aerospace_technologies_heating_systems.php (accessed April 1, 2016).

(21) http://www.vartechsystems.com/products/Transparent-Heaters.asp (accessed April 1, 2016).

(22) Laforte, J. L.; Allaire, M. A.; Laflamme, J. State-of-the-Art on Power Line De-Icing. *Atmos. Res.* **1998**, *46*, 143−158.

(23) http://www.frostfighter.com/clear-view-defrosters-about.htm (accessed April 1, 2016).

(24) https://www.plumbingsupply.com/clearmirrors.html (accessed April 1, 2016).

(25) http://www.marketsandmarkets.com/PressReleases/smart-glass.asp (accessed April 1, 2016).

(26) Kim, A. Y.; Lee, K.; Park, J. H.; Byun, D.; Lee, J. K. Double-Layer Effect on Electrothermal Properties of Transparent Heaters. *Phys. Status Solidi A* **2014**, *211*, 1923−1927.

(27) Yoon, Y. H.; Song, J. W.; Kim, D.; Kim, J.; Park, J. K.; Oh, S. K.; Han, C. S. Transparent Film Heater Using Single-Walled Carbon Nanotubes. *Adv. Mater.* **2007**, *19*, 4284−4287.

DOI: 10.1021/acsami.5b11026
ACS Appl. Mater. Interfaces 2016, 8, 12559−12575

(28) Celle, C.; Mayousse, C.; Moreau, E.; Basti, H.; Carella, A.; Simonato, J. P. Highly Flexible Transparent Film Heaters Based on Random Networks of Silver Nanowires. *Nano Res.* **2012**, *5*, 427−433.
(29) Woo, J. S.; Han, J. T.; Jung, S.; Jang, J. I.; Kim, H. Y.; Jeong, H. J.; Jeong, S. Y.; Baeg, K. J.; Lee, G. W. Electrically Robust Metal Nanowire Network Formation by in-Situ Interconnection with Single-Walled Carbon Nanotubes. *Sci. Rep.* **2014**, *4*, 4804.
(30) Rao, K. D. M.; Gupta, R.; Kulkarni, G. U. Fabrication of Large Area, High-Performance, Transparent Conducting Electrodes Using a Spontaneously Formed Crackle Network as Template. *Adv. Mater. Interfaces* **2014**, *1*, 1400090.
(31) Gupta, R.; Kulkarni, G. U. Holistic Method for Evaluating Large Area Transparent Conducting Electrodes. *ACS Appl. Mater. Interfaces* **2013**, *5*, 730−736.
(32) Kumar, A.; Kulkarni, G. U. Evaluating Conducting Network Based Transparent Electrodes from Geometrical Considerations. *J. Appl. Phys.* **2016**, *119*, 015102.
(33) Bae, J. J.; Lim, S. C.; Han, G. H.; Jo, Y. W.; Doung, D. L.; Kim, E. S.; Chae, S. J.; Huy, T. Q.; Luan, N. V. Heat Dissipation of Transparent Graphene Defoggers. *Adv. Funct. Mater.* **2012**, *22*, 4819−4826.
(34) Yang, K.; Cho, K.; Im, K.; Kim, S. Heat Generation Characteristics of Microheaters Prepared with ITO Nanoparticles and Organic Additives. *Mater. Res. Bull.* **2015**, *63*, 194−198.
(35) Kurdesau, F.; Khripunov, G.; da Cunha, A. F.; Kaelin, M.; Tiwari, A. N. Comparative Study of ITO Layers Deposited by DC and RFMagnetron Sputtering at Room Temperature. *J. Non-Cryst. Solids* **2006**, *352*, 1466−1470.
(36) Maruyama, T.; Fukui, K. Indium Tin Oxide Thin Films Prepared by Chemical Vapour Deposition. *Thin Solid Films* **1991**, *203*, 297−302.
(37) Rozati, S. M.; Ganj, T. Transparent Conductive Sn-Doped Indium Oxide Thin Films Deposited by Spray Pyrolysis Technique. *Renewable Energy* **2004**, *29*, 1671−1676.
(38) Ashida, T.; Miyamura, A.; Oka, N.; Sato, Y.; Yagi, T.; Taketoshi, N.; Baba, T.; Shigesato, Y. Thermal Transport Properties of Polycrystalline Tin-Doped Indium Oxide Films. *J. Appl. Phys.* **2009**, *105*, 073709.
(39) Im, K.; Cho, K.; Kim, J.; Kim, S. Transparent Heaters Based on Solution-Processed Indium Tin Oxide Nanoparticles. *Thin Solid Films* **2010**, *518*, 3960−3963.
(40) Im, K.; Cho, K.; Kwak, K.; Kim, J.; Kim, S. Flexible Transparent Heaters with Heating Films Made of Indium Tin Oxide Nanoparticles. *J. Nanosci. Nanotechnol.* **2013**, *13*, 3519−3521.
(41) Liu, D. S.; Sheu, C. S.; Lee, C. T.; Lin, C.-H. Thermal Stability of Indium Tin Oxide Thin Films Co-Sputtered with Zinc Oxide. *Thin Solid Films* **2008**, *516*, 3196−3203.
(42) Ahn, B. D.; Oh, S. H.; Hong, D. U.; Shin, D. H.; Moujoud, A.; Kim, H. J. Transparent Ga-Doped Zinc Oxide-Based Window Heaters Fabricated by Pulsed Laser Deposition. *J. Cryst. Growth* **2008**, *310*, 3303−3307.
(43) Kim, J. H.; Ahn, B. D.; Kim, C. H.; Jeon, K. A.; Kang, H. S.; Lee, S. Y. Heat Generation Properties of Ga Doped Zno Thin Films Prepared by RF-Magnetron Sputtering for Transparent Heaters. *Thin Solid Films* **2008**, *516*, 1330−1333.
(44) Gao, K. H.; Lin, T.; Liu, X. D.; Zhang, X. H.; Li, X. N.; Wu, J.; Liu, Y. F.; Wang, X. F.; Chen, Y. W.; Ni, B.; Dai, N.; Chu, J. H. Low Temperature Electrical Transport Properties of F-Doped SnO_2 Films. *Solid State Commun.* **2013**, *157*, 49−53.
(45) Hudaya, C.; Park, J. H.; Choi, W.; Lee, J. K. Characteristics of Fluorine-Doped Tin Oxide as a Transparent Heater on Pet Prepared by ECR-MOCVD. *ECS Trans.* **2013**, *53*, 161−166.
(46) Hudaya, C.; Jeon, B. J.; Lee, J. K. High Thermal Performance of SnO_2:F Thin Transparent Heaters with Scattered Metal Nanodots. *ACS Appl. Mater. Interfaces* **2015**, *7*, 57−61.
(47) Janas, D.; Koziol, K. K. A Review of Production Methods of Carbon Nanotube and Graphene Thin Films for Electrothermal Applications. *Nanoscale* **2014**, *6*, 3037−3045.
(48) Jung, D.; Han, M.; Lee, G. S. Flexible Transparent Conductive Heater Using Multiwalled Carbon Nanotube Sheet. *J. Vac. Sci. Technol., B: Microelectron. Nanometer Struct.-Process., Meas., Phenom.* **2014**, *32*, 04E105.
(49) Jang, H. S.; Jeon, S. K.; Nahm, S. H. The Manufacture of a Transparent Film Heater by Spinning Multi-Walled Carbon Nanotubes. *Carbon* **2011**, *49*, 111−116.
(50) Lee, K.; Scardaci, V.; Kim, H.-Y.; Hallam, T.; Nolan, H.; Bolf, B. E.; Maltbie, G. S.; Abbott, J. E.; Duesberg, G. S. Highly Sensitive, Transparent, and Flexible Gas Sensors Based on Gold Nanoparticle Decorated Carbon Nanotubes. *Sens. Actuators, B* **2013**, *188*, 571−575.
(51) Kang, J.; Kim, H.; Kim, K. S.; Lee, S. K.; Bae, S.; Ahn, J. H.; Kim, Y. J.; Choi, J. B.; Hong, B. H. High-Performance Graphene-Based Transparent Flexible Heaters. *Nano Lett.* **2011**, *11*, 5154−8.
(52) Sui, D.; Huang, Y.; Huang, L.; Liang, J.; Ma, Y.; Chen, Y. Flexible and Transparent Electrothermal Film Heaters Based on Graphene Materials. *Small* **2011**, *7*, 3186−3192.
(53) Bae, S.; Kim, H.; Lee, Y.; Xu, X.; Park, J. S.; Zheng, Y.; Balakrishnan, J.; Lei, T.; Ri Kim, H.; Song, Y. I.; Kim, Y. J.; Kim, K. S.; Ozymilmaz, B.; Ahn, J. H.; Hong, B. H.; Iijima, S. Roll-to-Roll Production of 30-Inch Graphene Films for Transparent Electrodes. *Nat. Nanotechnol.* **2010**, *5*, 574−578.
(54) Wang, J.; Fang, Z.; Zhu, H.; Gao, B.; Garner, S.; Cimo, P.; Barcikowski, Z.; Mignerey, A.; Hu, L. Flexible, Transparent, and Conductive Defrosting Glass. *Thin Solid Films* **2014**, *556*, 13−17.
(55) Chen, T. L.; Ghosh, D. S.; Marchena, M.; Osmond, J.; Pruneri, V. Nanopatterned Graphene on a Polymer Substrate by a Direct Peel-Off Technique. *ACS Appl. Mater. Interfaces* **2015**, *7*, 5938−5943.
(56) Wang, S.; Zhang, X.; Zhao, W. Flexible, Transparent, and Conductive Film Based on Random Networks of Ag Nanowires. *J. Nanomater.* **2013**, *2013*, 456098.
(57) Jiu, J. T.; Sugahara, T.; Nogi, M.; Suganuma, K. Ag Nanowires: Large-Scale Synthesis Via a Trace-Salt-Assisted Solvothermal Process and Application in Transparent Electrodes. *J. Nanopart. Res.* **2013**, *15*, 1588.
(58) Sun, Y. G.; Xia, Y. N. Large-Scale Synthesis of Uniform Silver Nanowires through a Soft, Self-Seeding, Polyol Process. *Adv. Mater.* **2002**, *14*, 833−837.
(59) Lee, J. H.; Lee, P.; Lee, D.; Lee, S. S.; Ko, S. H. Large-Scale Synthesis and Characterization of Very Long Silver Nanowires Via Successive Multistep Growth. *Cryst. Growth Des.* **2012**, *12*, 5598−5605.
(60) Sun, Y.; Mayers, B.; Herricks, T.; Xia, Y. Polyol Synthesis of Uniform Silver Nanowires: A Plausible Growth Mechanism and the Supporting Evidence. *Nano Lett.* **2003**, *3*, 955−960.
(61) Madaria, A.; Kumar, A.; Ishikawa, F.; Zhou, C. Uniform, Highly Conductive, and Patterned Transparent Films of a Percolating Silver Nanowire Network on Rigid and Flexible Substrates Using a Dry Transfer Technique. *Nano Res.* **2010**, *3*, 564−573.
(62) Hu, L. B.; Kim, H. S.; Lee, J. Y.; Peumans, P.; Cui, Y. Scalable Coating and Properties of Transparent, Flexible, Silver Nanowire Electrodes. *ACS Nano* **2010**, *4*, 2955−2963.
(63) Scardaci, V.; Coull, R.; Lyons, P. E.; Rickard, D.; Coleman, J. N. Spray Deposition of Highly Transparent, Low-Resistance Networks of Silver Nanowires over Large Areas. *Small* **2011**, *7*, 2621−2628.
(64) Leem, D. S.; Edwards, A.; Faist, M.; Nelson, J.; Bradley, D. D. C.; de Mello, J. C. Efficient Organic Solar Cells with Solution-Processed Silver Nanowire Electrodes. *Adv. Mater.* **2011**, *23*, 4371−4375.
(65) Larciprete, M. C.; Albertoni, A.; Belardini, A.; Leahu, G.; Li Voti, R.; Mura, F.; Sibilia, C.; Nefedov, I.; Anoshkin, I. V.; Kauppinen, E. I.; Nasibulin, A. G. Infrared Properties of Randomly Oriented Silver Nanowires. *J. Appl. Phys.* **2012**, *112*, 083503.
(66) Kim, D.; Zhu, L.; Jeong, D. J.; Chun, K.; Bang, Y. Y.; Kim, S. R.; Kim, J. H.; Oh, S. K. Transparent Flexible Heater Based on Hybrid of Carbon Nanotubes and Silver Nanowires. *Carbon* **2013**, *63*, 530−536.
(67) Kim, T.; Kim, Y. W.; Lee, H. S.; Kim, H.; Yang, W. S.; Suh, K. S. Uniformly Interconnected Silver-Nanowire Networks for Transparent Film Heaters. *Adv. Funct. Mater.* **2013**, *23*, 1250−1255.

DOI: 10.1021/acsami.5b11026
ACS Appl. Mater. Interfaces 2016, 8, 12559−12575

(68) Khaligh, H. H.; Goldthorpe, I. A. Failure of Silver Nanowire Transparent Electrodes under Current Flow. *Nanoscale Res. Lett.* **2013**, *8*, 235.
(69) Li, Y.; Tsuchiya, K.; Tohmyoh, H.; Saka, M. Numerical Analysis of the Electrical Failure of a Metallic Nanowire Mesh Due to Joule Heating. *Nanoscale Res. Lett.* **2013**, *8*, 370.
(70) Gupta, R.; Walia, S.; Hösel, M.; Jensen, J.; Angmo, D.; Krebs, F. C.; Kulkarni, G. U. Solution Processed Large Area Fabrication of Ag Patterns as Electrodes for Flexible Heaters, Electrochromics and Organic Solar Cells. *J. Mater. Chem. A* **2014**, *2*, 10930−10937.
(71) Seong, B.; Yoo, H.; Nguyen, V. D.; Jang, Y.; Ryu, C.; Byun, D. Metal-Mesh Based Transparent Electrode on a 3-D Curved Surface by Electrohydrodynamic Jet Printing. *J. Micromech. Microeng.* **2014**, *24*, 097002.
(72) Gao, T.; Wang, B.; Ding, B.; Lee, J. K.; Leu, P. W. Uniform and Ordered Copper Nanomeshes by Microsphere Lithography for Transparent Electrodes. *Nano Lett.* **2014**, *14*, 2105−2110.
(73) Wu, H.; Kong, D.; Ruan, Z.; Hsu, P.-C.; Wang, S.; Yu, Z.; Carney, T. J.; Hu, L.; Fan, S.; Cui, Y. A Transparent Electrode Based on a Metal Nanotrough Network. *Nat. Nanotechnol.* **2013**, *8*, 421−425.
(74) Han, B.; Pei, K.; Huang, Y.; Zhang, X.; Rong, Q.; Lin, Q.; Guo, Y.; Sun, T.; Guo, C.; Carnahan, D.; Giersig, M.; Wang, Y.; Gao, J.; Ren, Z.; Kempa, K. Uniform Self-Forming Metallic Network as a High-Performance Transparent Conductive Electrode. *Adv. Mater.* **2014**, *26*, 873−877.
(75) Kiruthika, S.; Rao, K. D. M.; Kumar, A.; Gupta, R.; Kulkarni, G. U. Metal Wire Network Based Transparent Conducting Electrodes Fabricated Using Interconnected Crackled Layer as Template. *Mater. Res. Express* **2014**, *1*, 026301.
(76) Gupta, R.; Rao, K. D.; Srivastava, K.; Kumar, A.; Kiruthika, S.; Kulkarni, G. U. Spray Coating of Crack Templates for the Fabrication of Transparent Conductors and Heaters on Flat and Curved Surfaces. *ACS Appl. Mater. Interfaces* **2014**, *6*, 13688−13696.
(77) Rao, K. D. M.; Hunger, C.; Gupta, R.; Kulkarni, G. U.; Thelakkat, M. A Cracked Polymer Templated Metal Network as a Transparent Conducting Electrode for ITO-Free Organic Solar Cells. *Phys. Chem. Chem. Phys.* **2014**, *16*, 15107−15110.
(78) Li, Y. A.; Chen, Y. J.; Tai, N. H. Highly Thermal Conductivity and Infrared Emissivity of Flexible Transparent Film Heaters Utilizing Silver-Decorated Carbon Nanomaterials as Fillers. *Mater. Res. Express* **2014**, *1*, 025605.
(79) Zhang, X.; Yan, X.; Chen, J.; Zhao, J. Large-Size Graphene Microsheets as a Protective Layer for Transparent Conductive Silver Nanowire Film Heaters. *Carbon* **2014**, *69*, 437−443.
(80) Lee, S. M.; Lee, J. H.; Bak, S.; Lee, K.; Li, Y.; Lee, H. Hybrid Windshield-Glass Heater for Commercial Vehicles Fabricated Via Enhanced Electrostatic Interactions Among a Substrate, Silver Nanowires, and an Over-Coating Layer. *Nano Res.* **2015**, *8*, 1882−1892.
(81) Cheong, H. G.; Song, D. W.; Park, J. W. Transparent Film Heaters with Highly Enhanced Thermal Efficiency Using Silver Nanowires and Metal/Metal-Oxide Blankets. *Microelectron. Eng.* **2015**, *146*, 11−18.
(82) Kwon, N.; Kim, K.; Heo, J.; Yi, I.; Chung, I. Study on Ag Mesh/Conductive Oxide Hybrid Transparent Electrode for Film Heaters. *Nanotechnology* **2014**, *25*, 265702.
(83) Ji, S.; He, W.; Wang, K.; Ran, Y.; Ye, C. Thermal Response of Transparent Silver Nanowire/PEDOT:PSS Film Heaters. *Small* **2014**, *10*, 4951−4960.
(84) Hunger, C.; Rao, K. D. M.; Gupta, R.; Singh, C. R.; Kulkarni, G. U.; Thelakkat, M. Transparent Metal Network with Low Haze and High Figure of Merit Applied to Front and Back Electrodes in Semitransparent ITO-Free Polymer Solar Cells. *Energy Technol.* **2015**, *3*, 638−645.
(85) Li, J.; Liang, J.; Jian, X.; Hu, W.; Li, J.; Pei, Q. A Flexible and Transparent Thin Film Heater Based on a Silver Nanowire/Heat-Resistant Polymer Composite. *Macromol. Mater. Eng.* **2014**, *299*, 1403−1409.
(86) Lu, H. Y.; Chou, C. Y.; Wu, J. H.; Lin, J. J.; Liou, G. S. Highly Transparent and Flexible Polyimide-AgNW Hybrid Electrodes with Excellent Thermal Stability for Electrochromic Applications and Defogging Devices. *J. Mater. Chem. C* **2015**, *3*, 3629−3635.
(87) Li, M.; Ji, S.; Pan, J.; Wu, H.; Zhong, L.; Wang, Q.; Li, F.; Li, G. Infrared Response of Self-Heating VO_2 Nanoparticles Film Based on Ag Nanowires Heater. *J. Mater. Chem. A* **2014**, *2*, 20470−20473.
(88) Kang, J.; Jang, Y.; Kim, Y.; Cho, S. H.; Suhr, J.; Hong, B. H.; Choi, J. B.; Byun, D. Ag-Grid/Graphene Hybrid Structure for Large-Scale, Transparent, Flexible Heaters. *Nanoscale* **2015**, *7*, 6567−6573.
(89) Preston, C.; Xu, Y.; Han, X.; Munday, J. N.; Hu, L. Optical Haze of Transparent and Conductive Silver Nanowire Films. *Nano Res.* **2013**, *6*, 461−468.
(90) Kim, T.; Canlier, A.; Cho, C.; Rozyyev, V.; Lee, J. Y.; Han, S. M. Highly Transparent Au-Coated Ag Nanowire Transparent Electrode with Reduction in Haze. *ACS Appl. Mater. Interfaces* **2014**, *6*, 13527−13534.
(91) Hosseinzadeh Khaligh, H.; Goldthorpe, I. A. Hot-Rolling Nanowire Transparent Electrodes for Surface Roughness Minimization. *Nanoscale Res. Lett.* **2014**, *9*, 1−5.
(92) Nam, S.; Song, M.; Kim, D. H.; Cho, B.; Lee, H. M.; Kwon, J. D.; Park, S. G.; Nam, K.-S.; Jeong, Y.; Kwon, S. H.; Park, Y. C.; Jin, S. H.; Kang, J. W.; Jo, S.; Kim, C. S. Ultrasmooth, Extremely Deformable and Shape Recoverable Ag Nanowire Embedded Transparent Electrode. *Sci. Rep.* **2014**, *4*, 4788.
(93) Liu, Y.; Chang, Q.; Huang, L. Transparent, Flexible Conducting Graphene Hybrid Films with a Subpercolating Network of Silver Nanowires. *J. Mater. Chem. C* **2013**, *1*, 2970−2974.
(94) Jing, M. X.; Han, C.; Li, M.; Shen, X. Q. High Performance of Carbon Nanotubes/Silver Nanowires-PET Hybrid Flexible Transparent Conductive Films Via Facile Pressing-Transfer Technique. *Nanoscale Res. Lett.* **2014**, *9*, 1−7.
(95) Rao, K. D. M.; Kulkarni, G. U. A Highly Crystalline Single Au Wire Network as a High Temperature Transparent Heater. *Nanoscale* **2014**, *6*, 5645−5651.
(96) Kiruthika, S.; Gupta, R.; Anand, A.; Kumar, A.; Kulkarni, G. U. Fabrication of Oxidation-Resistant Metal Wire Network-Based Transparent Electrodes by a Spray-Roll Coating Process. *ACS Appl. Mater. Interfaces* **2015**, *7*, 27215−27222.
(97) Nian, Q.; Saei, M.; Xu, Y.; Sabyasachi, G.; Deng, B.; Chen, Y. P.; Cheng, G. J. Crystalline Nanojoining Silver Nanowire Percolated Networks on Flexible Substrate. *ACS Nano* **2015**, *9*, 10018−10031.
(98) Kang, T. J.; Kim, T.; Seo, S. M.; Park, Y. J.; Kim, Y. H. Thickness-Dependent Thermal Resistance of a Transparent Glass Heater with a Single-Walled Carbon Nanotube Coating. *Carbon* **2011**, *49*, 1087−1093.
(99) Gupta, R.; Kulkarni, G. U. Holistic Method for Evaluating Large Area Transparent Conducting Electrodes. *ACS Appl. Mater. Interfaces* **2013**, *5*, 730−736.
(100) Sorel, S.; Bellet, D.; Coleman, J. N. Relationship between Material Properties and Transparent Heater Performance for Both Bulk-Like and Percolative Nanostructured Networks. *ACS Nano* **2014**, *8*, 4805−4814.
(101) Chen, T. L.; Ghosh, D. S.; Marchena, M.; Osmond, J.; Pruneri, V. Nanopatterned Graphene on a Polymer Substrate by a Direct Peel-Off Technique. *ACS Appl. Mater. Interfaces* **2015**, *7*, 5938−5943.
(102) Kiruthika, S.; Gupta, R.; Kulkarni, G. U. Large Area Defrosting Windows Based on Electrothermal Heating of Highly Conducting and Transmitting Ag Wire Mesh. *RSC Adv.* **2014**, *4*, 49745−49751.
(103) Jang, H. S.; Jeon, S. K.; Kwon, O. H.; Lee, S. C.; Kim, C. S.; Nahm, S. H. Growth of Spin-Capable Multi-Walled Carbon Nanotubes and Flexible Transparent Sheet Films. *J. Nanosci. Nanotechnol.* **2012**, *12*, 3242−3246.
(104) Hong, S.; Lee, H.; Lee, J.; Kwon, J.; Han, S.; Suh, Y. D.; Cho, H.; Shin, J.; Yeo, J.; Ko, S. K. Highly Stretchable and Transparent Metal Nanowire Heater for Wearable Electronics Applications. *Adv. Mater.* **2015**, *27*, 4744−4751.

DOI: 10.1021/acsami.5b11026
ACS Appl. Mater. Interfaces 2016, 8, 12559−12575

(105) Wu, Z. P.; Wang, J. N. Preparation of Large-Area Double-Walled Carbon Nanotube Films and Application as Film Heater. *Phys. E* **2009**, *42*, 77−81.
(106) Thomas, S. K.; Cassoni, R. P.; MacArthur, C. D. Aircraft Anti-Icing and De-Icing Techniques and Modeling. *J. Aircr.* **1996**, *33*, 841−854.
(107) Jung, D.; Kim, D.; Lee, K. H.; Overzet, L. J.; Lee, G. S. Transparent Film Heaters Using Multi-Walled Carbon Nanotube Sheets. *Sens. Actuators, A* **2013**, *199*, 176−180.
(108) Kim, D.; Lee, E.; Lee, H. S.; Yoon, J. Energy Efficient Glazing for Adaptive Solar Control Fabricated with Photothermotropic Hydrogels Containing Graphene Oxide. *Sci. Rep.* **2015**, *5*, 7646.
(109) Long, L.; Ye, H. How to Be Smart and Energy Efficient: A General Discussion on Thermochromic Windows. *Sci. Rep.* **2014**, *4*, 6427.
(110) Zhou, J.; Gao, Y.; Zhang, Z.; Luo, H.; Cao, C.; Chen, Z.; Dai, L.; Liu, X. VO_2 Thermochromic Smart Window for Energy Savings and Generation. *Sci. Rep.* **2013**, *3*, 3029.
(111) Kim, H.; Kim, Y.; Kim, K. S.; Jeong, H. Y.; Jang, A. R.; Han, S. H.; Yoon, D. H.; Suh, K. S.; Shin, H. S.; Kim, T.; Yang, W. S. Flexible Thermochromic Window Based on Hybridized VO_2/Graphene. *ACS Nano* **2013**, *7*, 5769−5776.
(112) Cooney, C. G.; Towe, B. C. A Thermopneumatic Dispensing Micropump. *Sens. Actuators, A* **2004**, *116*, 519−524.
(113) Yeung, S. W.; Lee, T. M. H.; Cai, H.; Hsing, I. M. A DNA Biochip for on-the-Spot Multiplexed Pathogen Identification. *Nucleic Acids Res.* **2006**, *34*, e118.
(114) Webb, R. C.; Bonifas, A. P.; Behnaz, A.; Zhang, Y.; Yu, K. J.; Cheng, H.; Shi, M.; Bian, Z.; Liu, Z.; Kim, Y.-S.; Yeo, W.-H.; Park, J. S.; Song, J.; Li, Y.; Huang, Y.; Gorbach, A. M.; Rogers, J. A. Ultrathin Conformal Devices for Precise and Continuous Thermal Characterization of Human Skin. *Nat. Mater.* **2013**, *12*, 938−944.
(115) Gao, L.; Zhang, Y.; Malyarchuk, V.; Jia, L.; Jang, K. I.; Chad Webb, R.; Fu, H.; Shi, Y.; Zhou, G.; Shi, L.; Shah, D.; Huang, X.; Xu, B.; Yu, C.; Huang, Y.; Rogers, J. A. Epidermal Photonic Devices for Quantitative Imaging of Temperature and Thermal Transport Characteristics of the Skin. *Nat. Commun.* **2014**, *5*, 4938.
(116) Moschou, D.; Vourdas, N.; Kokkoris, G.; Papadakis, G.; Parthenios, J.; Chatzandroulis, S.; Tserepi, A. All-Plastic, Low-Power, Disposable, Continuous-Flow PCR Chip with Integrated Microheaters for Rapid DNA Amplification. *Sens. Actuators, B* **2014**, *199*, 470−478.
(117) Liu, P.; Liu, L.; Jiang, K.; Fan, S. Carbon-Nanotube Film Microheater on a Polyethylene Terephthalate Substrate and Its Application in Thermochromic Displays. *Small* **2011**, *7*, 732−736.
(118) Khan, U.; Kim, T. H.; Lee, K. H.; Lee, J. H.; Yoon, H. J.; Bhatia, R.; Sameera, I.; Seung, W.; Ryu, H.; Falconi, C.; Kim, S. W. Self-Powered Transparent Flexible Graphene Microheaters. *Nano Energy* **2015**, *17*, 356−365.
(119) Choi, H.; Choi, J. S.; Kim, J.-S.; Choe, J.-H.; Chung, K. H.; Shin, J. W.; Kim, J. T.; Youn, D. H.; Kim, K. C.; Lee, J. I.; Choi, S. Y.; Kim, P.; Choi, C. G.; Yu, Y. J. Flexible and Transparent Gas Molecule Sensor Integrated with Sensing and Heating Graphene Layers. *Small* **2014**, *10*, 3685−3691.
(120) Walia, S.; Gupta, R.; Kulkarni, G. U. Disposable Heater Arrays Using Printed Ag Patterns on Polyethylene Terephthalate for Multipurpose Applications. *Energy Technol.* **2015**, *3*, 359−365.
(121) Barron, S. C.; Gorham, J. M.; Patel, M. P.; Green, M. L. High-Throughput Measurements of Thermochromic Behavior in $V_{1-X}Nb_xO_2$ Combinatorial Thin Film Libraries. *ACS Comb. Sci.* **2014**, *16*, 526−534.
(122) Hsu, P. C.; Liu, X.; Liu, C.; Xie, X.; Lee, H. R.; Welch, A. J.; Zhao, T.; Cui, Y. Personal Thermal Management by Metallic Nanowire-Coated Textile. *Nano Lett.* **2015**, *15*, 365−371.
(123) Choi, H.; Choi, J. S.; Kim, J. S.; Choe, J. H.; Chung, K. H.; Shin, J. W.; Kim, J. T.; Youn, D. H.; Kim, K. C.; Lee, J. I.; Choi, S. Y.; Kim, P.; Choi, C. G.; Yu, Y. J. Flexible Electronics: Flexible and Transparent Gas Molecule Sensor Integrated with Sensing and Heating Graphene Layers. *Small* **2014**, *10*, 3812.
(124) http://xefro.com/ (accessed April 1, 2016).

DOI: 10.1021/acsami.5b11026
ACS Appl. Mater. Interfaces 2016, 8, 12559−12575